NASA TECHNICAL NOTE

NASA TN D-4228

A MOVING-BELT GROUND PLANE FOR WIND-TUNNEL GROUND SIMULATION AND RESULTS FOR TWO JET-FLAP CONFIGURATIONS

by Thomas R. Turner

Langley Research Center
Langley Station, Hampton, Va.

NATIONAL AERONAUTICS AND SPACE ADMINISTRATION • WASHINGTON, D. C. • NOVEMBER 1967

A MOVING-BELT GROUND PLANE FOR WIND-TUNNEL GROUND SIMULATION AND RESULTS FOR TWO JET-FLAP CONFIGURATIONS

By Thomas R. Turner

Langley Research Center
Langley Station, Hampton, Va.

NATIONAL AERONAUTICS AND SPACE ADMINISTRATION

For sale by the Clearinghouse for Federal Scientific and Technical Information
Springfield, Virginia 22151 – CFSTI price $3.00

A MOVING-BELT GROUND PLANE FOR WIND-TUNNEL GROUND SIMULATION AND RESULTS FOR TWO JET-FLAP CONFIGURATIONS

By Thomas R. Turner
Langley Research Center

SUMMARY

A moving-belt ground plane designed to eliminate the ground boundary layer for tests in ground proximity has been installed in a 17-foot (5.18-meter) wind-tunnel test section at the Langley Research Center. The test section has been calibrated with this moving belt installed, and the effects of ground proximity on the characteristics of a swept and an unswept full-span blowing-flap configuration have been investigated.

The results indicate that the moving belt satisfactorily removes the boundary layer on the ground plane. The lift loss of models at small distances from the ground and high lifts is considerably less with the belt moving at stream velocity (boundary layer removed) than with the belt at zero velocity. For configurations with full-span lift devices, the data indicate that the moving-belt ground plane is not needed for ratios of wing height (in spans) to lift coefficient greater than about 0.050, but is desirable for smaller ratios.

INTRODUCTION

In wind-tunnel investigations of ground effects, the ground is normally simulated by placing a board in the airstream immediately below the model. This type of ground board effectively divides the tunnel into two air passages so that the determination of the dynamic pressure is complicated. In addition, the ground simulation is not strictly correct because a boundary layer develops between the airstream and the ground board. This boundary layer has not been a serious problem in tests of conventional (low lift) aircraft models. However, the advent of very high-lift devices, such as blowing and jet flaps, created renewed interest in wind-tunnel ground simulation since these high-lift models showed very large lift losses as the ground board was approached. Reference 1 gives the results for an investigation in which a model was tested in a wind tunnel over a conventional ground board and was tested also by moving it over the ground to determine how much of the lift loss was due to ground proximity and how much was due to the presence of the boundary layer on the tunnel ground board. These results showed that the apparent lift loss due to ground proximity, for high-lift configurations, can be much too

large when obtained over a conventional wind-tunnel ground board and indicated the need for a better system of simulating the ground in wind-tunnel testing. The concept of a ground plane moving at the tunnel stream velocity was considered an accurate means of simulating the ground in wind-tunnel testing. A moving-belt installation at the Langley Research Center, together with early test results obtained therewith, was discussed in reference 2. Similar devices developed in England, France, and Germany have been reported in references 3 to 6.

The purpose of the present report is to describe the design and operational details of the moving-belt ground plane installed in the 17-foot (5.18-meter) test section of the Langley 300-mph 7- by 10-foot tunnel. Data for two blowing-flap models tested over the moving belt are also presented.

SYMBOLS

b	span, meters
C_D	drag coefficient, $\frac{\text{Drag}}{q_\infty S}$
C_L	lift coefficient, $\frac{\text{Lift}}{q_\infty S}$
C_m	pitching-moment coefficient, $\frac{\text{Pitching moment}}{q_\infty S\bar{c}}$
C_μ	momentum coefficient, $\frac{\text{Static thrust (flap off)}}{q_\infty S}$
c	local chord
$\bar{c}$	mean aerodynamic chord, meters
h	wing height, meters (see figs. 7 and 8)
q	local dynamic pressure, newtons/meter^2
q_∞	free-stream dynamic pressure, newtons/meter^2
S	area, meters^2
V	local velocity, meters/sec
V_∞	free-stream velocity, meters/sec

V_B belt velocity, meters/sec

α angle of attack, degrees

δ_f flap deflection, degrees

δ_s leading-edge slat deflection, degrees

θ effective wake deflection angle, degrees

THE MOVING-BELT GROUND-PLANE SYSTEM

The Moving Belt

The 3.66-meter-wide by 3.05-meter-long moving-belt ground plane was built and installed in a 17-foot (5.18-meter) test section (ref. 7) in the entrance bell to the Langley 300-mph 7- by 10-foot tunnel. The moving-belt ground plane was mounted on the tunnel floor because it was simpler mechanically to position a model above the ground plane than to fix a model near the vertical center of a test section and move the ground plane up and down beneath the model. The tunnel-floor mount also eliminates the split test section and its resultant problems in determining dynamic pressure.

The moving-belt ground-plane system installed in the 17-foot (5.18-meter) test section is shown in figure 1. The moving-belt system, including the model mount and boundary-layer removal system, is shown in figure 1(a). Figure 1(b) shows the plan view for the belt system installed on the test-section floor with the drive system outside of the test section. The belt is made of 0.476-centimeter-thick woven wool impregnated with a plastic to keep air from passing through it and is supported by two uncrowned rollers and a polished aluminum backing plate. The 19.06-centimeter-diameter rollers are solid dural except for stainless-steel end caps and shaft to take self-alining ball bearings. The polished rollers were dynamically balanced well above the operating range. The idler (front) roller is adjustable upstream and downstream for adjusting the belt tension and belt tracking. The rollers are several centimeters wider than the belt, and thus give the belt room to move toward either end as the speed is varied. If it moves too far before stabilizing at a given speed, the tension is manually changed on one edge of the belt. In general, the belt moves away from the tighter side. Guides have been installed on the edges of the backup plate just ahead of the drive (rear) roller and on the tunnel floor just back of the idler (front) roller to make the belt tracking less sensitive to belt tension and idler (front) roller skew. The guides consist of ball bearings stacked

on a rod and mounted in such a manner that the effective diameter of the drive (rear) roller increases as the end is approached.

The backup plate with the 20 suction chambers and high-pressure blowing orifices is shown in figure 2. Any combination of the suction chambers can be manifolded so that suction can be applied to local areas when needed to lessen the tendency of the belt to float above the backup plate. The high-pressure holes (lines) were installed so that high-pressure air could be pumped between the belt and backup plate to form an air bearing and to act as a coolant in case the belt ran hot because of friction on the backup plate (fig. 2). Fortunately, no heating problem has developed, so this cooling system has not been needed.

The drive system consists of a 30-horsepower (22.4-kilowatt) 1770-rpm alternating-current motor coupled through a magnetic clutch and a timing belt to the downstream (rear) roller of the belt rig. The belt velocity is controllable from 0 to 30.5 meters per second. In operation the belt runs with no hump at the rollers and with no noticeable waviness or ripples over the backup plate.

A 2.54-centimeter suction slot extends the width of the belt ahead of the upstream roller to remove the boundary layer up to this point. (See fig. 1(a).) The plate forming the upper boundary of this slot and fairing with the belt has two rows of suction holes at its trailing edge which extend full width and are connected to the suction slot to remove boundary layer on this plate. The suction slot is ducted back into the test section of the Langley 300-mph 7- by 10-foot tunnel located downstream of the 17-foot test section, and the boundary layer is pumped off because of the lower pressure of this higher velocity test section.

Model Support

The model support system allows an angle-of-attack range from -10° to 30° (except when limited by the sting or model touching the belt at the lower ground heights) and allows for a sideslip-angle range from -25° to 25° (fig. 1(a)). The model height above the ground plane can be remotely varied for 91.5 centimeters ($\alpha = 0^{\circ}$) by the telescoping strut. Strut extensions are available for greater model heights from the belt, with the same 91.5-centimeter remotely variable height.

The vertical part of the model mounting strut moves over a considerable area of the tunnel floor downstream of the belt in covering the angle-of-attack and sideslip range. To avoid any sizable opening in the tunnel, a section of the tunnel floor was replaced with a large cross tunnel rollup door in the center of which a small streamwise rollup door was installed. The strut is installed through a clearance hole at the center of this small door. The doors are driven by the strut as it moves to the desired angle (fig. 1(b)).

Flow Surveys With Moving-Belt Rig Installed

A rather large divergence of the test-section sidewalls (fig. 1(b)) was required to obtain satisfactory velocity gradients at the test-section center line when the 17-foot test section was built into the Langley 300-mph 7- by 10-foot tunnel circuit (ref. 7). A preliminary survey over the belt reflected this divergence in a decrease in dynamic pressure in the downstream direction with the belt either moving or not moving. Installation of wedge-shape fairings (fig. 1(a)) in the troughs between the moving-belt rig and the tunnel sidewalls considerably decreased the velocity gradient. With this fairing installed, a rather complete dynamic-pressure survey was made over the moving-belt ground plane with the belt moving and not moving. The 3.66-meter-long, 4.45-centimeter-diameter static probe used for the survey had orifices spaced 15.24 centimeters apart. Typical dynamic-pressure plots are presented in figures 3 and 4 with the belt not operating; however, operating the belt has no effect on the velocity gradient outside the boundary layer of the belt. The total streamwise variation in dynamic pressure over the belt is approximately 4 percent of average pressure; however, the variation in dynamic pressure from station 120 centimeters to station 240 centimeters, the normal model position, is less than 1 percent of average pressure (fig. 3). The dynamic pressure changes only slightly at a lateral distance of 114 centimeters from the tunnel center line. The vertical dynamic-pressure gradient is negligible from 0 to 100 centimeters above the belt in the model test location but decreases by approximately 3 percent as the height is increased from 100 to 240 centimeters, the highest position normally used for testing (fig. 4).

As mentioned previously, the belt is made of woven wool and, consequently, the surface is somewhat soft and fuzzy. A surface with such a texture causes the boundary layer to build up faster than a hard, smooth-textured surface. A comparison of the velocity ratio over the belt at station 142.0 centimeters and over a smooth metal plate placed on the belt is shown in figure 5. For V/V_∞ ratios of 0.9 or above, the boundary layer on the belt at station 142.0 centimeters is approximately twice as thick as that on the flat metal plate. With the belt in operation (fig. 6), the boundary-layer thickness over the belt is reduced as the belt velocity is increased and has zero thickness at a belt velocity approximately equal to free-stream velocity. With further increase in belt velocity, the air velocity very near the belt becomes greater than free-stream velocity (fig. 6).

CHARACTERISTICS OF MODELS TESTED OVER MOVING-BELT GROUND PLANE

Models

An investigation of two models provided with high-lift devices was made over the moving-belt ground plane to determine its effectiveness in simulating the ground in

wind-tunnel testing. This investigation was made at a free-stream dynamic pressure of 191.5 newtons per square meter. One model was an unswept wing with a full-span blowing flap. Some details of the model are shown in figure 7 and further details are given in reference 1. The data for this model were corrected for the tare of the unshielded part of the air-supply tube and mounting strut. The large moment transfer (fig. 7) probably affects the accuracy of the pitching-moment data presented for this model. For this model the height h above the moving belt was measured from the chord plane.

The other model used in this investigation was a wing-fuselage configuration with the wing swept back 35°. This wing (fig. 8) was made to the same specifications and dimensions as the semispan wing shown in figure 1 of reference 8. The full-span leading-edge slat and trailing-edge flap were fixed at 60° for this investigation. For this model the distance h was measured from the lower surface at the quarter chord (fig. 8). The blowing-flap slot or gap was designed to have the same spanwise variation as the wing chord, and the wing plenum was to maintain a constant pressure along the flap span. Construction difficulties and inaccuracies resulted in a nonuniform slot gap and a variable plenum pressure across the flap span. These conditions made it impossible to compute accurate blowing momentum coefficients C_{μ}; consequently, the data for the swept-wing configuration are presented for various lift coefficients for the model at $\alpha = 0^{\circ}$ and at a height of 0.613 span above the moving-belt ground plane, the greatest height used for this model. The operating reference pressure for the various lift coefficients was taken from a plot of C_L as a function of flap blowing reference pressure for the model at $\alpha = 0^{\circ}$ and a height of 0.61 span.

Results

Unswept-wing data.- The results for the unswept wing over the moving-belt ground plane are presented in figure 9 for flap-deflection angles from 15° to 75°. The coefficients C_L, C_D, and C_m are plotted against C_{μ} for $\alpha = 0^{\circ}$ and for several heights above the ground with the belt velocity at zero and at free-stream velocity. The lift loss from ground influence at the high lift coefficients is considerably decreased with the belt moving at tunnel stream velocity. Variations of aerodynamic coefficients with angle of attack in ground proximity for several conditions are presented in figure 10.

A comparison of the ratio of lift in ground proximity to lift out of ground proximity for the belt at zero velocity and free-stream velocity for the unswept wing at $\alpha = 0^{\circ}$, $C_{\mu} = 3.5$, and $\delta_f = 60^{\circ}$ is shown in figure 11. Results for this same model taken from reference 1 for a conventional ground board and a moving model are also shown in this figure. The moving-belt ground-plane data with zero belt velocity compare reasonably well with the conventional ground board data. The agreement between the data for the

moving model and the data for the moving-belt ground plane is fair only. In view of the complexities involved in the moving-model technique of obtaining data, it is believed that the data obtained over the moving-belt ground plane are more reliable.

Swept-wing data.- Results for the 35^{o} swept-wing model over the moving-belt ground plane are presented in figure 12. The leading-edge slat and full-span blowing flap were deflected 60^{o} for these data. Lift, drag, and pitching-moment coefficients plotted against angle of attack are presented in figure 12 for lift coefficients varying from 0.50 to 8.03 for $h/b = 0.61$ and $\alpha = 0^{o}$. These initial lift coefficients, except for $C_L = 0.50$ (fig. 12(a)) were obtained by blowing over the flap. The lift increment due to operating the moving-belt ground plane at stream velocity for the condition shown in figure 12(c) appears to have the wrong sign; however, since no error has been found in the data this variation must remain unexplained.

In general, the lift increment between the moving-belt ground plane at free-stream velocity and zero velocity (conventional ground board) is dependent on configuration, lift coefficient, angle of attack, and flap-blowing-momentum coefficient.

Factors determining use of moving-belt ground plane.- Figure 13 is a graph which shows under what conditions it is desirable (based on lift characteristics) to have a moving-belt ground plane for wind-tunnel testing of models with full-span lift devices. The data points are from the models of this investigation and reference 2. The points are for the lift value at which the lift curve for zero belt velocity and the lift curve for free-stream belt velocity diverge for a given height in spans. The solid line in the figure is the height above the ground computed for a given lift coefficient by assuming that the effective deflection angle θ for the stream tube impinges on the ground a distance of 2.5 spans downstream from the model. It should be noted that θ is equal to one-half the deflection calculated from momentum theory (refs. 2 and 9). The stream tube-deflection angle θ is the complement of the wake skew angle used in reference 9. The agreement between the data points and the curve (line) is interesting, and it is also interesting to note that the downstream distance of 2.5 spans is almost the same as the impingement distance at which recirculation effects in the wind tunnel begin to produce noticeable effects on the data (ref. 9). The conventional wind-tunnel ground board is satisfactory for full-span lift configurations having lift and height combinations above the boundary or data points, that is, ratios of h/b to C_L greater than about 0.050 (fig. 13). For lift and height combinations below the boundary, a moving-belt ground plane is desirable.

As observed, the results presented in this report are for configurations with the lift distributed across the full span. The results presented in reference 2 for configurations having their lift concentrated in discrete jets (for example, direct-jet VTOL configurations) indicate that the moving-belt ground plane is not required.

CONCLUDING REMARKS

A moving-belt ground plane has been installed in a wind tunnel and the airflow over the ground plane has been calibrated. The calibration shows that the moving belt reduces the ground boundary-layer thickness to (practically) zero and does not increase existing velocity gradients in the test section.

The lift loss from ground influence for two models investigated over the moving belt at low heights and high lift coefficients is less with the belt at stream velocity than with the belt at zero velocity. This investigation indicated that the conventional wind-tunnel ground board is satisfactory for ratios of wing height (in spans) to lift coefficient greater than about 0.050 for configurations with full-span lift devices. For such ratios smaller than about 0.050 the moving-belt ground plane is desirable.

Langley Research Center,
National Aeronautics and Space Administration,
Langley Station, Hampton, Va., May 17, 1967,
721-01-00-16-23.

REFERENCES

1. Turner, Thomas R.: Ground Influence on a Model Airfoil With a Jet-Augmented Flap as Determined by Two Techniques. NASA TN D-658, 1961.

2. Turner, Thomas R.: Endless-Belt Technique for Ground Simulation. Conference on V/STOL and STOL Aircraft, NASA SP-116, 1966, pp. 435-446.

3. Butler, S. F. J.; Moy, B. A.; and Hutchins, G. D.: Low-Speed Tunnel Tests of an Aspect-Ratio 9 Jet-Flap Model, With Ground Simulation by Moving-Belt Rig. C.P. No. 849, Brit. A.R.C., 1966.

4. Werlé, Henri: Simulation de L'Effet de Sol au Tunnel Hydrodynamique (Ground-Effect Simulation at the Water-Tunnel). La Rech. Aérospatiale, no. 95, July-Aug. 1963, pp. 7-15.

5. Schlichting, H.; and Gersten, K.: Discussion on Aerodynamic Aspects of V/STOL Aeroplanes. DFL-Ber. Nr. 151, Deut. Forschungsanstalt Luftfahrt e.V., 1961.

6. Löhr, R.: Erhöhung des Maximalauftriebes eines Rechteckflügels in Bodennähe durch kombiniertes Ausblasen an der Flügelnase und an der Hinterkantenklappe. DLR FB 64-02, Deut. Luft- und Raumfahrt, April 1964.

7. Kuhn, Richard E.; and Hayes, William C., Jr.: Wind-Tunnel Investigation of Longitudinal Aerodynamic Characteristics of Three Propeller-Driven VTOL Configurations in the Transition Speed Range, Including Effects of Ground Proximity. NASA TN D-55, 1960.

8. Turner, Thomas R.: Low-Speed Investigation of a Full-Span Internal-Flow Jet-Augmented Flap on a High-Wing Model With a 35° Swept Wing of Aspect Ratio 7.0. NASA TN D-434, 1960.

9. Heyson, Harry H.; and Grunwald, Kalman J.: Wind-Tunnel Boundary Interference for V/STOL Testing. Conference on V/STOL and STOL Aircraft, NASA SP-116, 1966, pp. 409-434.

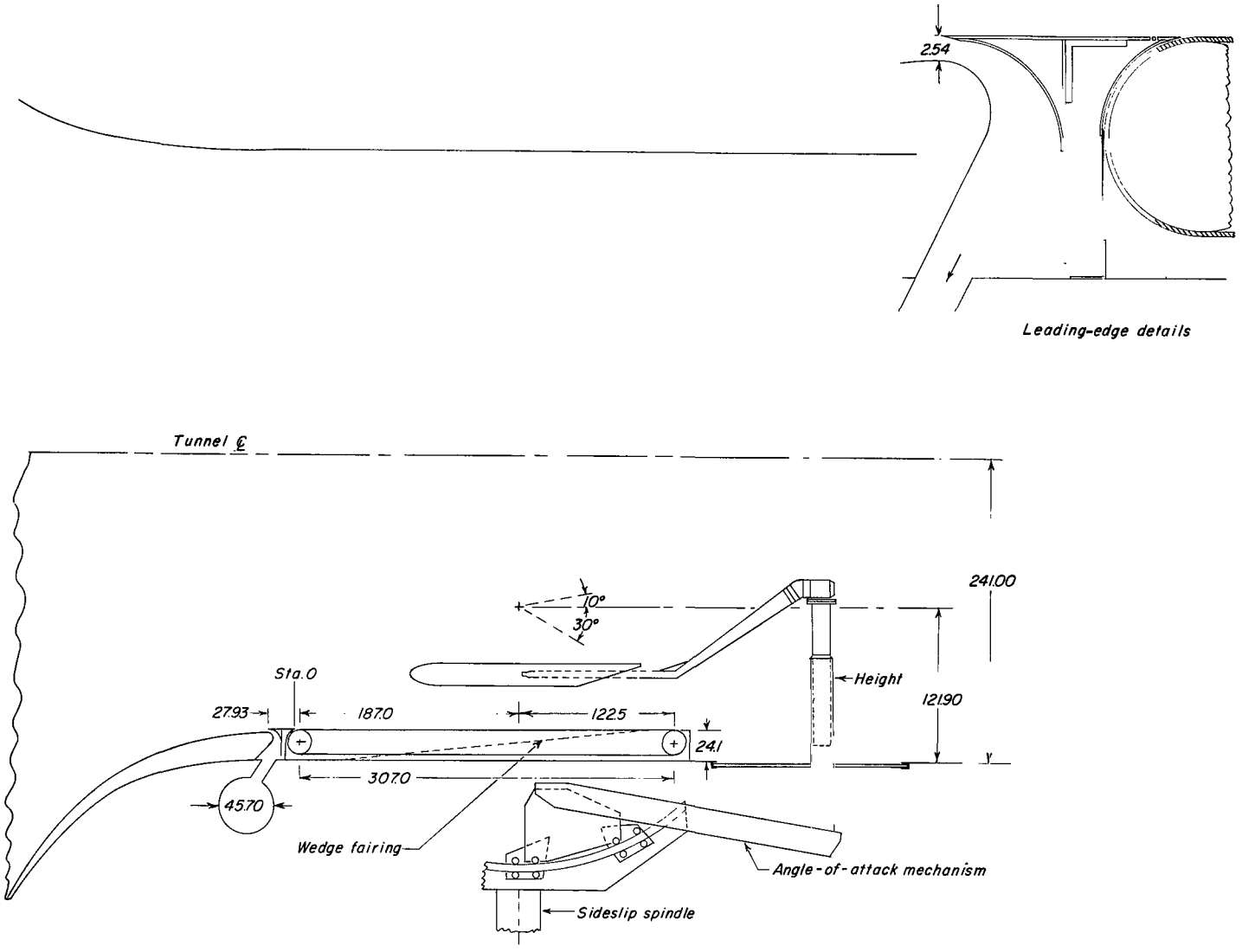

(a) Elevation.

Figure 1.- Drawing of moving-belt ground plane. Dimensions in centimeters except as noted.

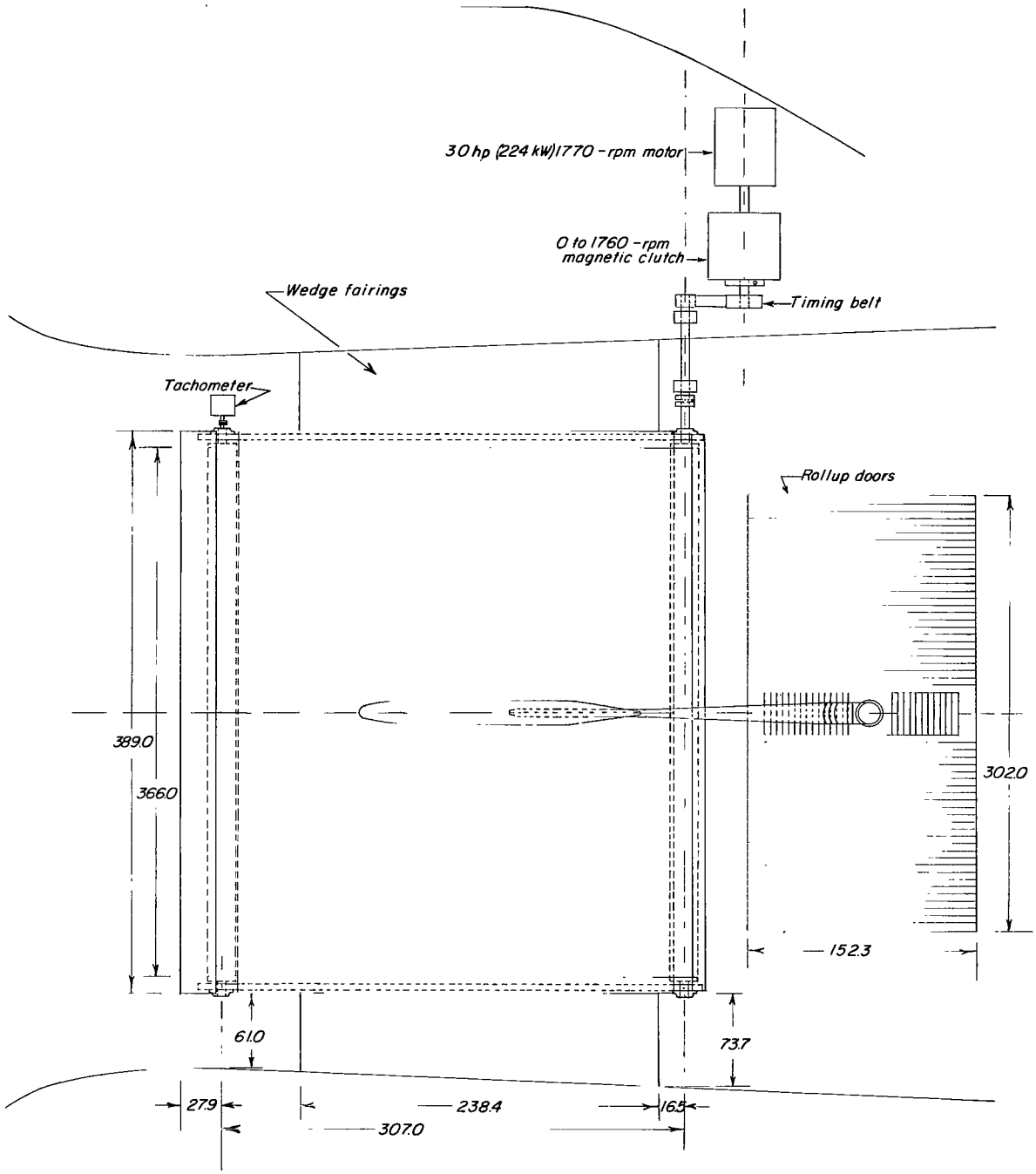

(b) Plan.

Figure 1.- Concluded.

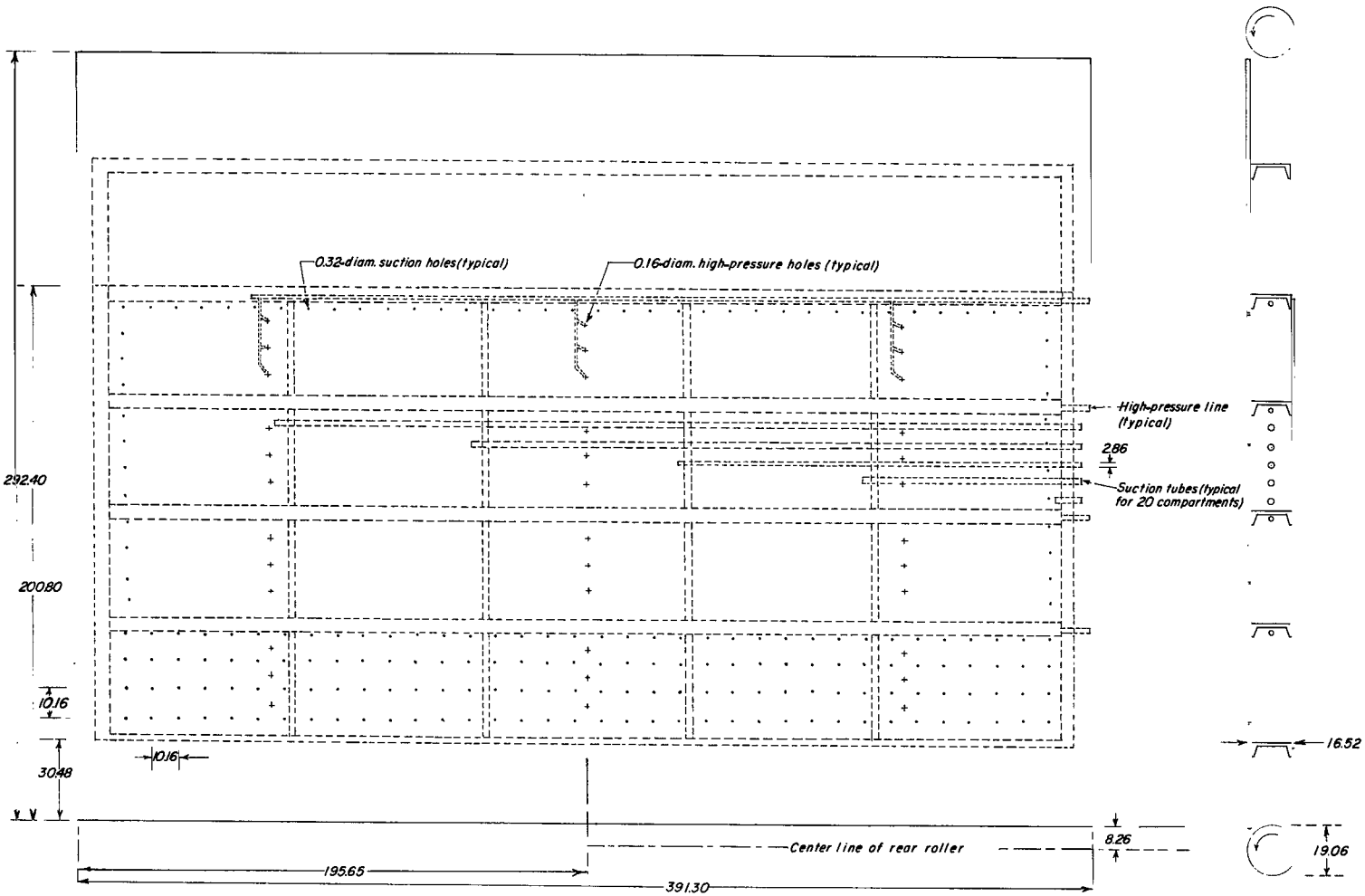

Figure 2.- Moving-belt ground plane backup plate. Dimensions in centimeters except as noted.

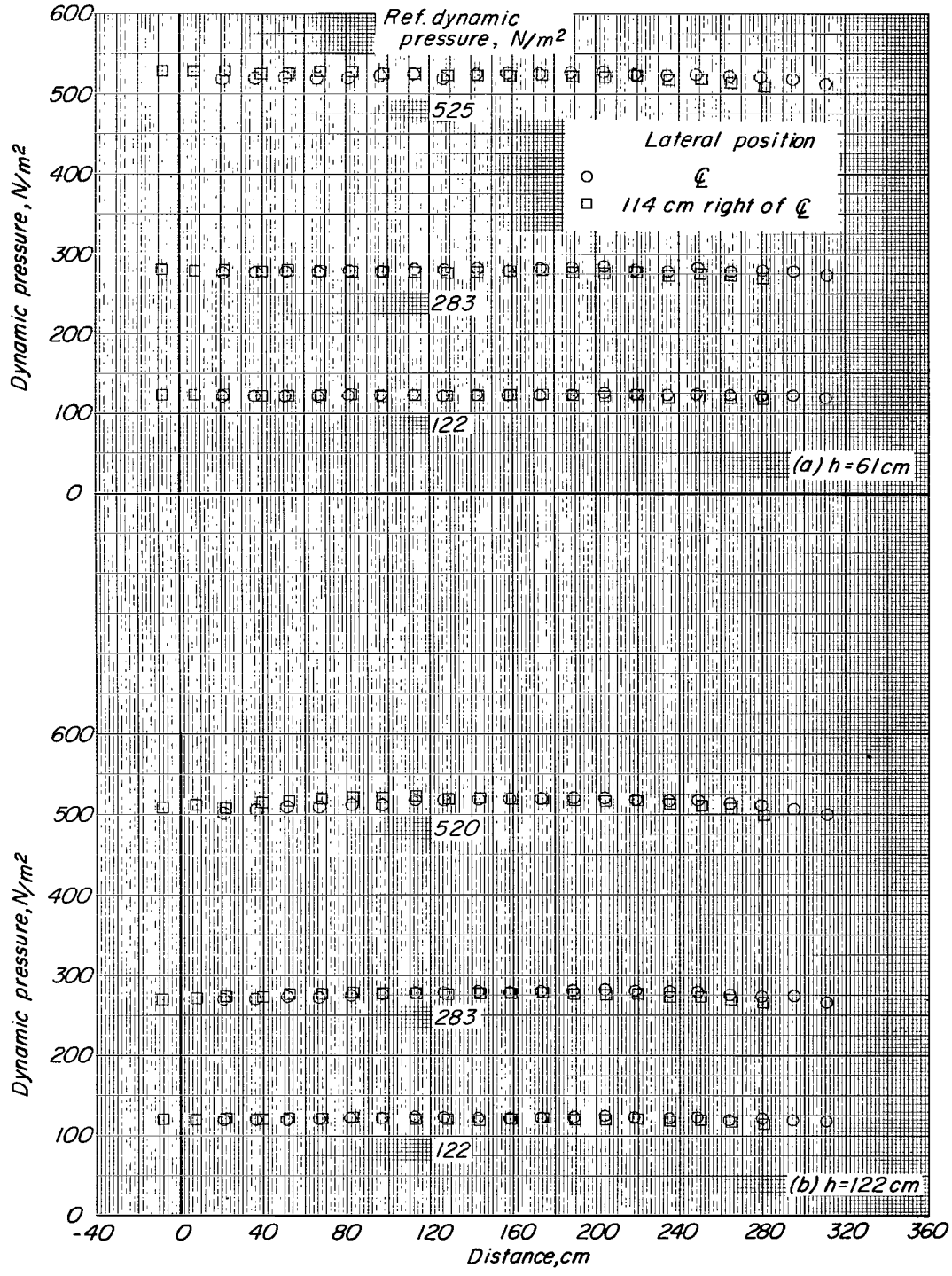

Figure 3.- Streamwise dynamic-pressure distribution over belt. Zero belt velocity.

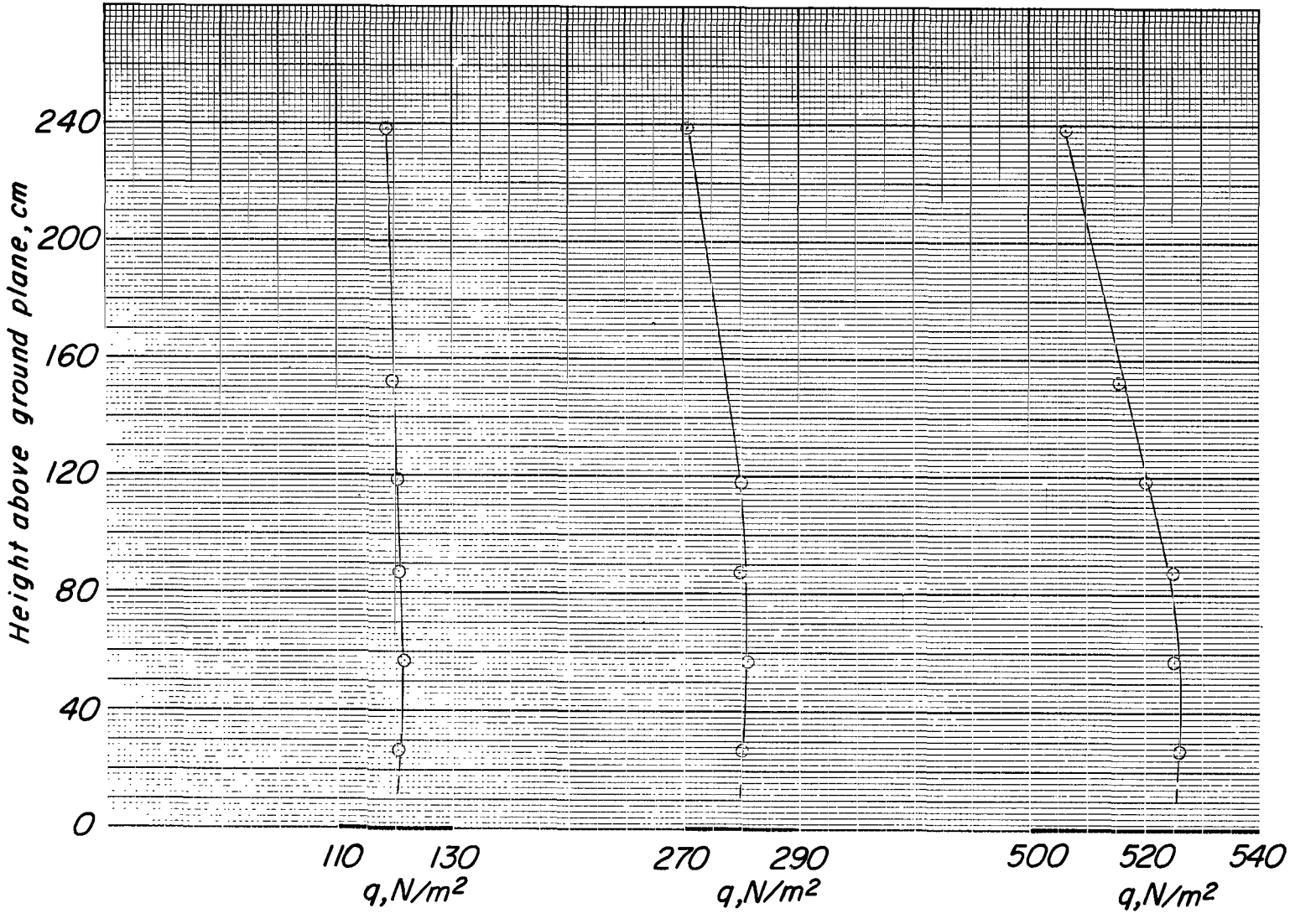

Figure 4.- Vertical dynamic-pressure variation over belt at model pivot location and lateral center line. Zero belt velocity.

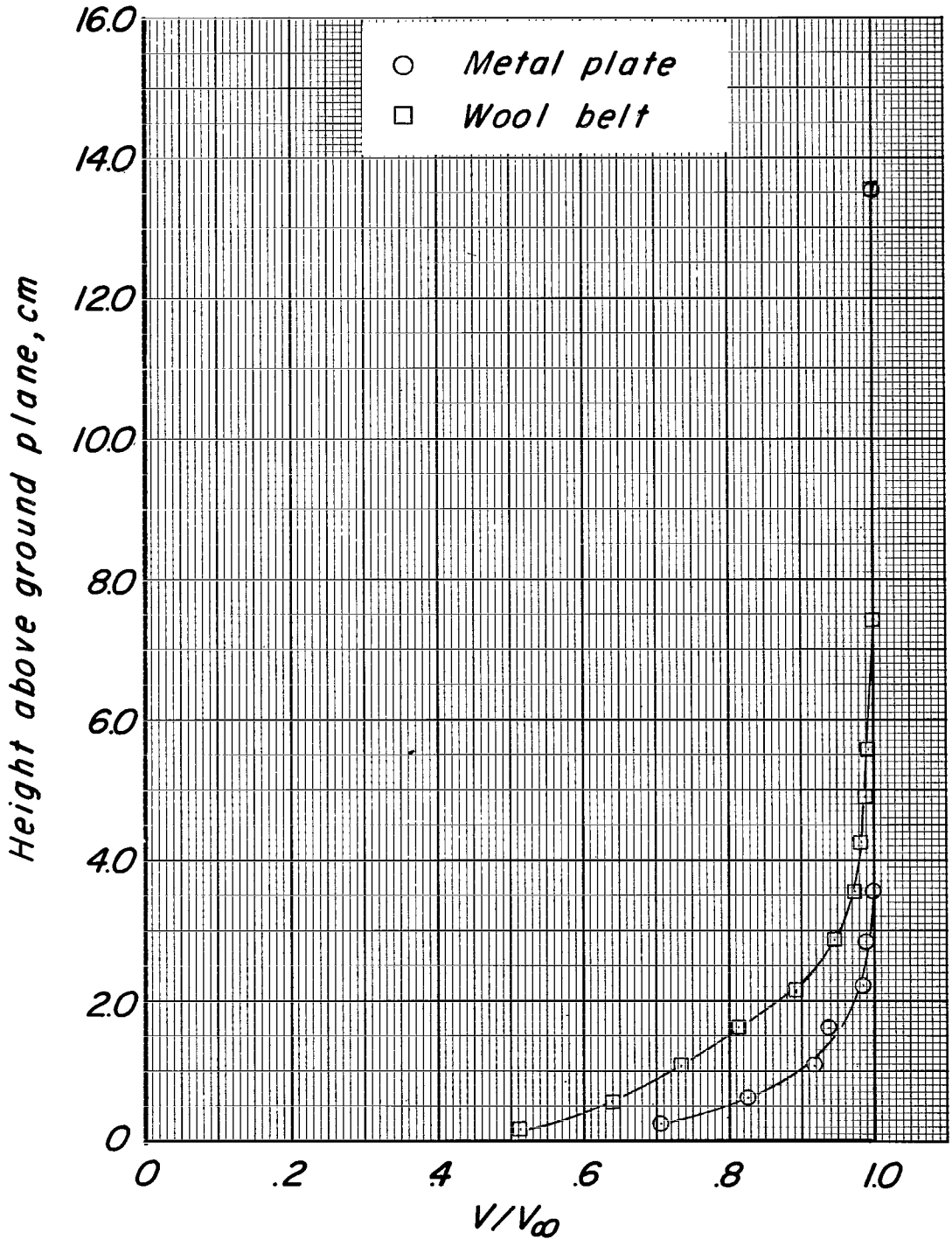

Figure 5.- Boundary-layer profile on belt and on smooth metal plate. Station 142.0 cm; zero belt velocity.

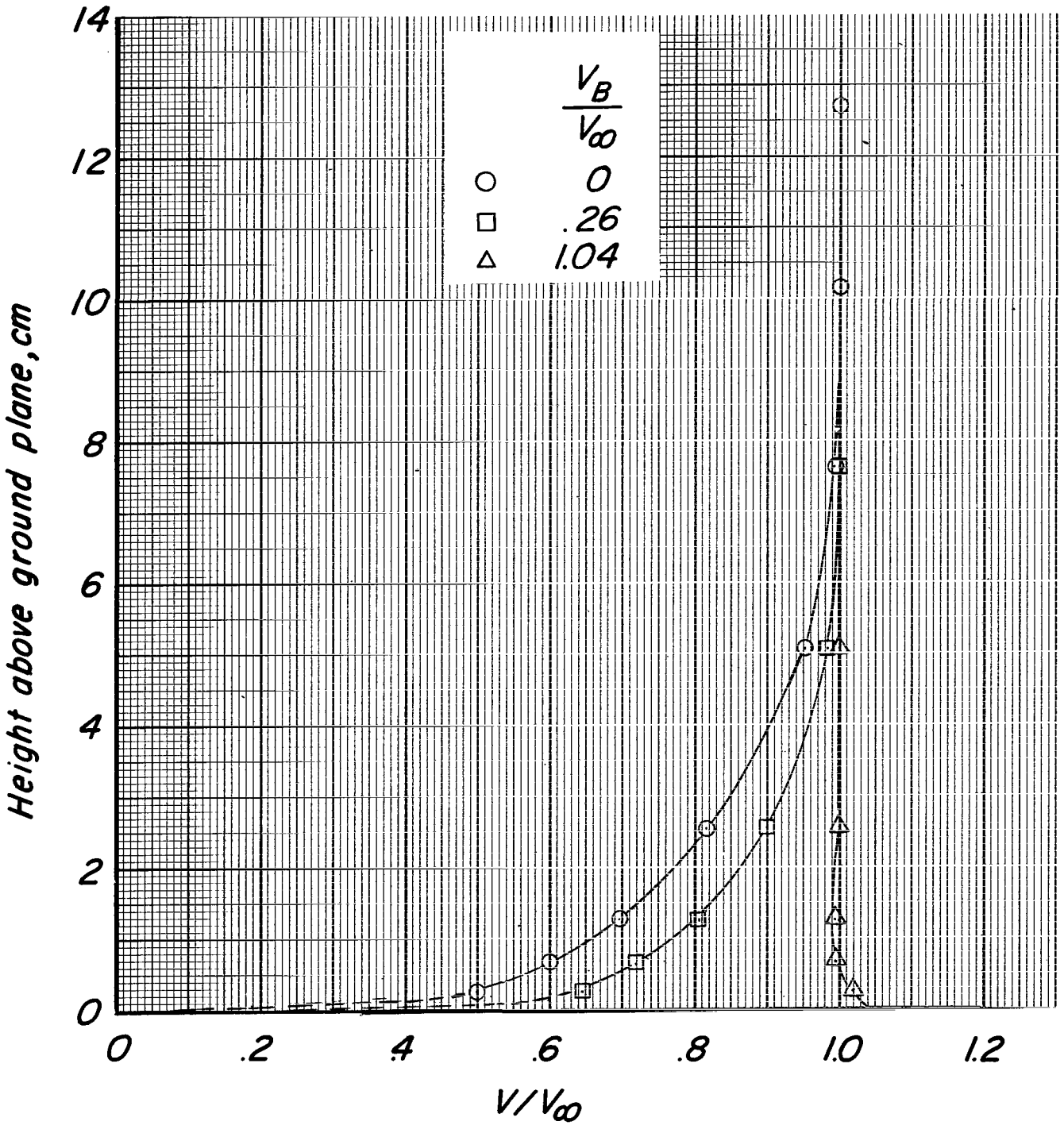

Figure 6.- Effect of belt velocity on boundary-layer profile. Station 187.0 cm.

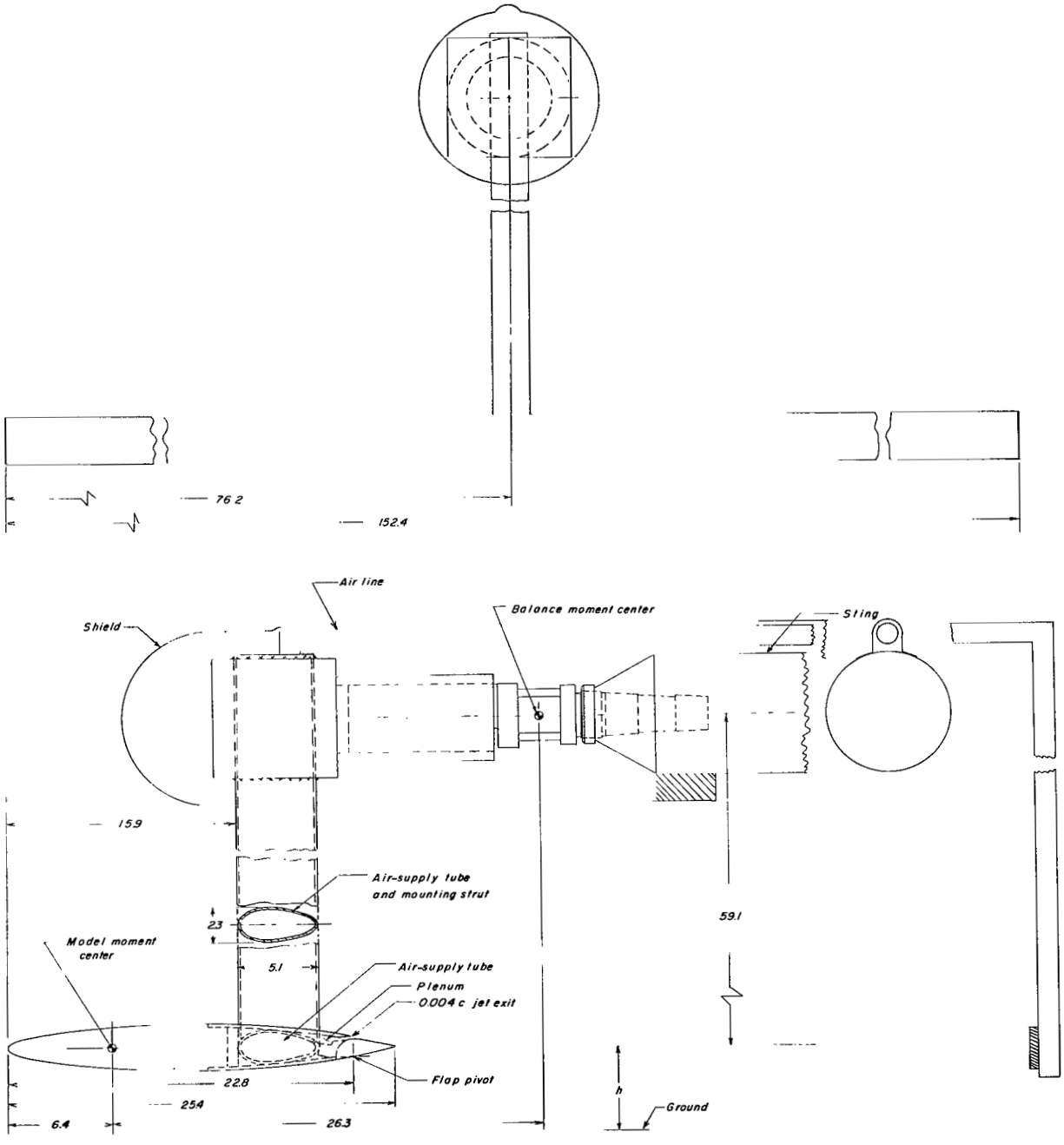

Figure 7.- Drawing of model and strain-gage-balance mounting. Dimensions are in centimeters unless otherwise noted.

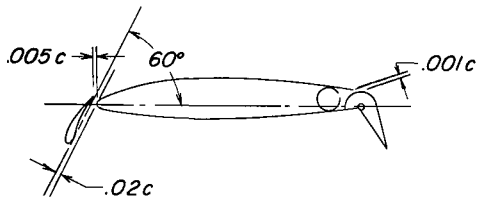

Typical wing cross section (streamwise) showing leading-edge and trailing-edge flaps deflected. (Not to scale.)

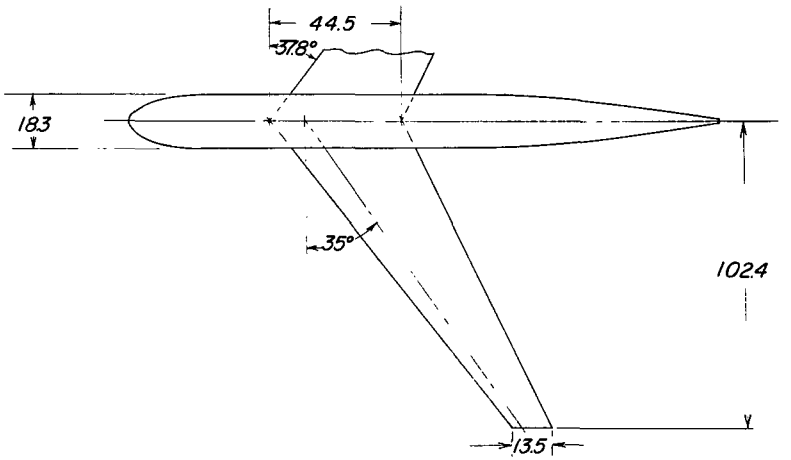

Wing	
Aspect ratio	7.0
Span	204.8 cm
Area	.594 m^2
Root chord	44.5 cm
Mean aerodynamic chord	31.8 cm
Airfoil section (parallel to airstream)	
Root section	65A 414
Tip section	65A 410
Leading-edge sweep	37.83°
Incidence	0°

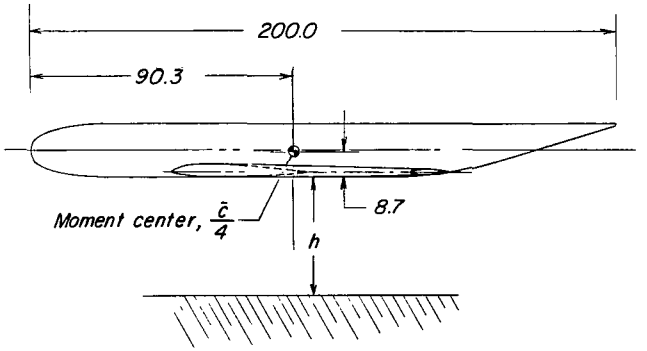

Figure 8.- Drawing of the 35° swept-wing model with full-span blowing flap. Dimensions in centimeters except as noted.

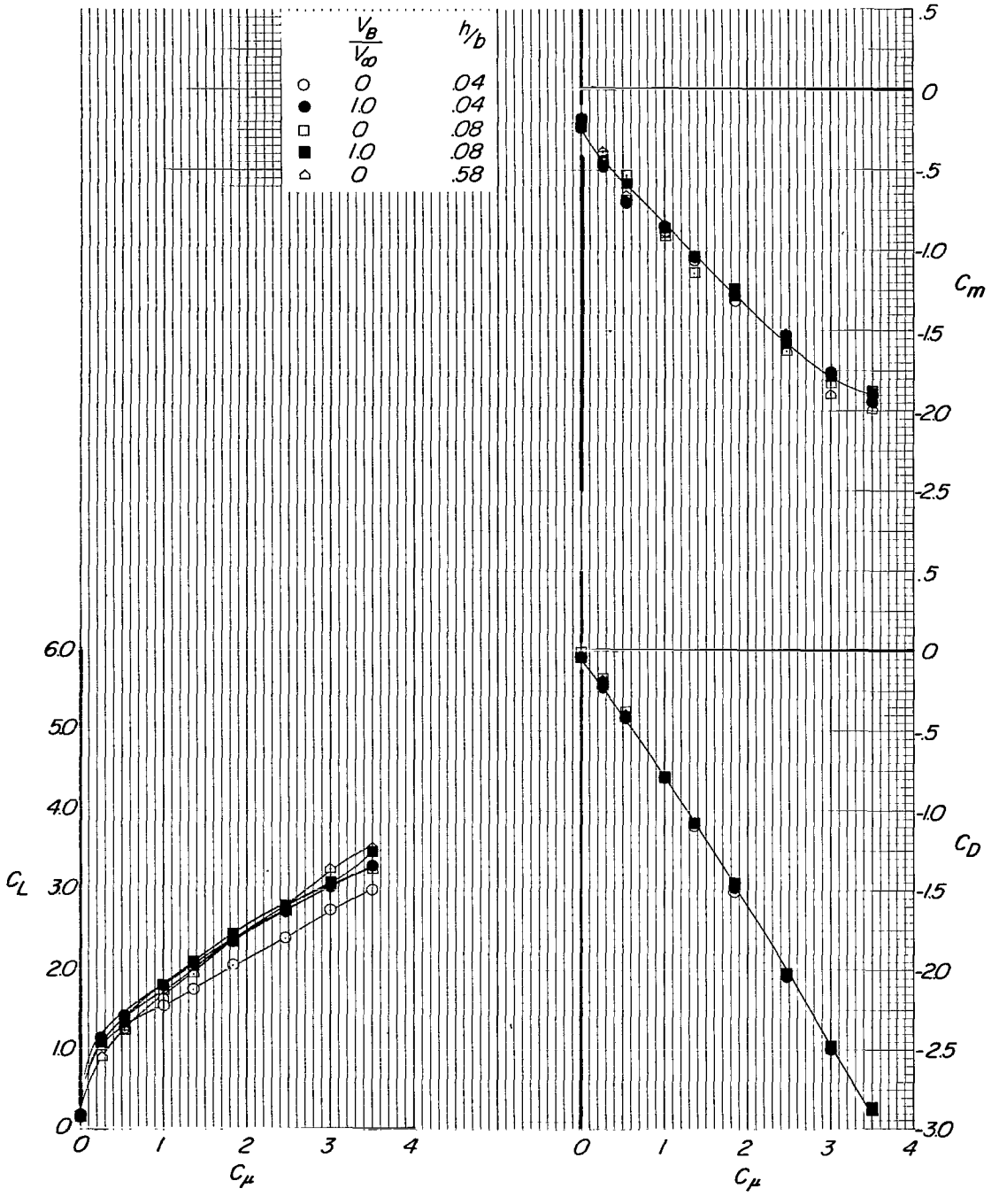

(a) $\delta_f = 15^0$.

Figure 9.- Variation of aerodynamic characteristics of unswept airfoil with C_μ at various heights above moving-belt ground plane. $\alpha = 0^0$.

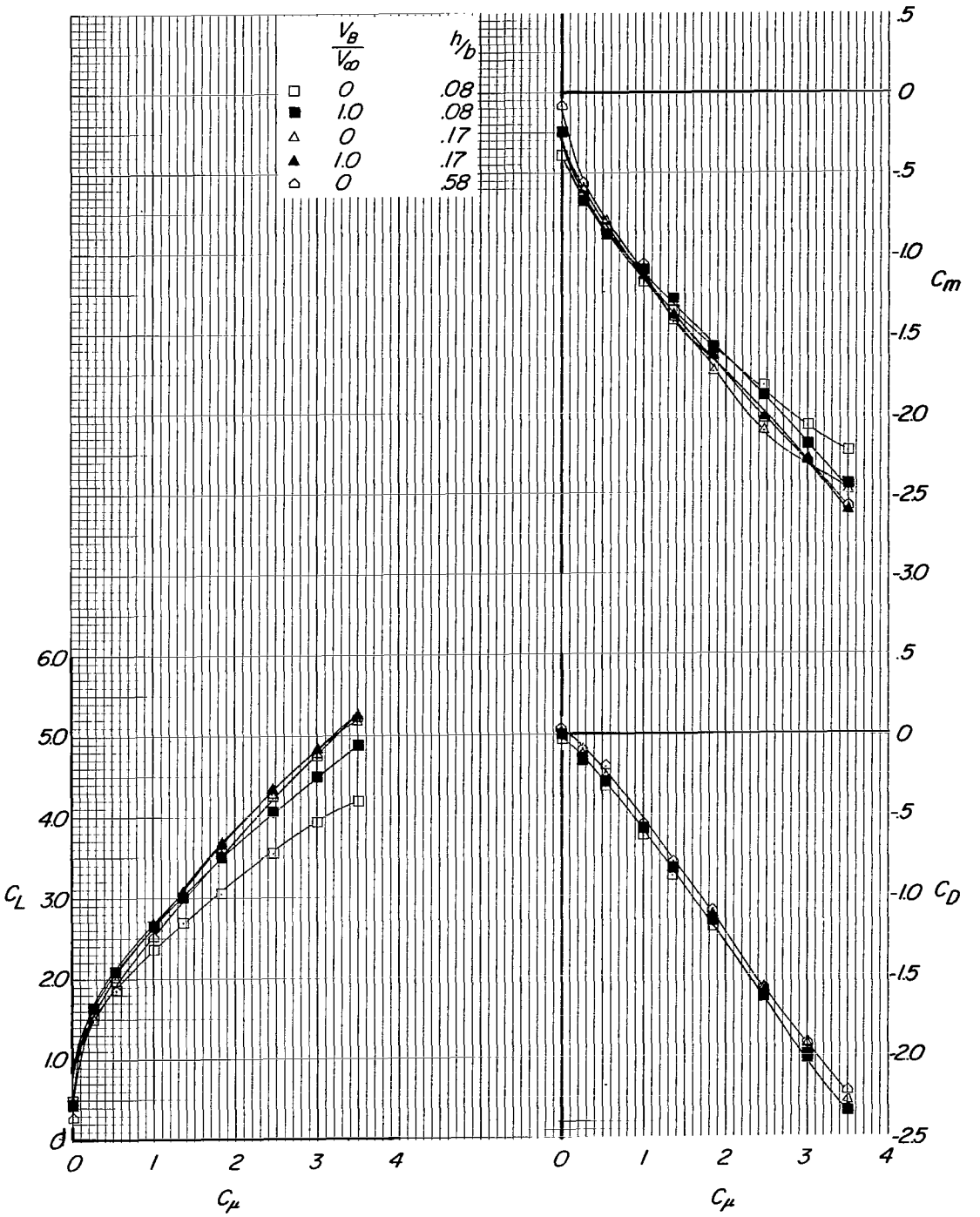

(b) $\delta_f = 30^o$.

Figure 9.- Continued.

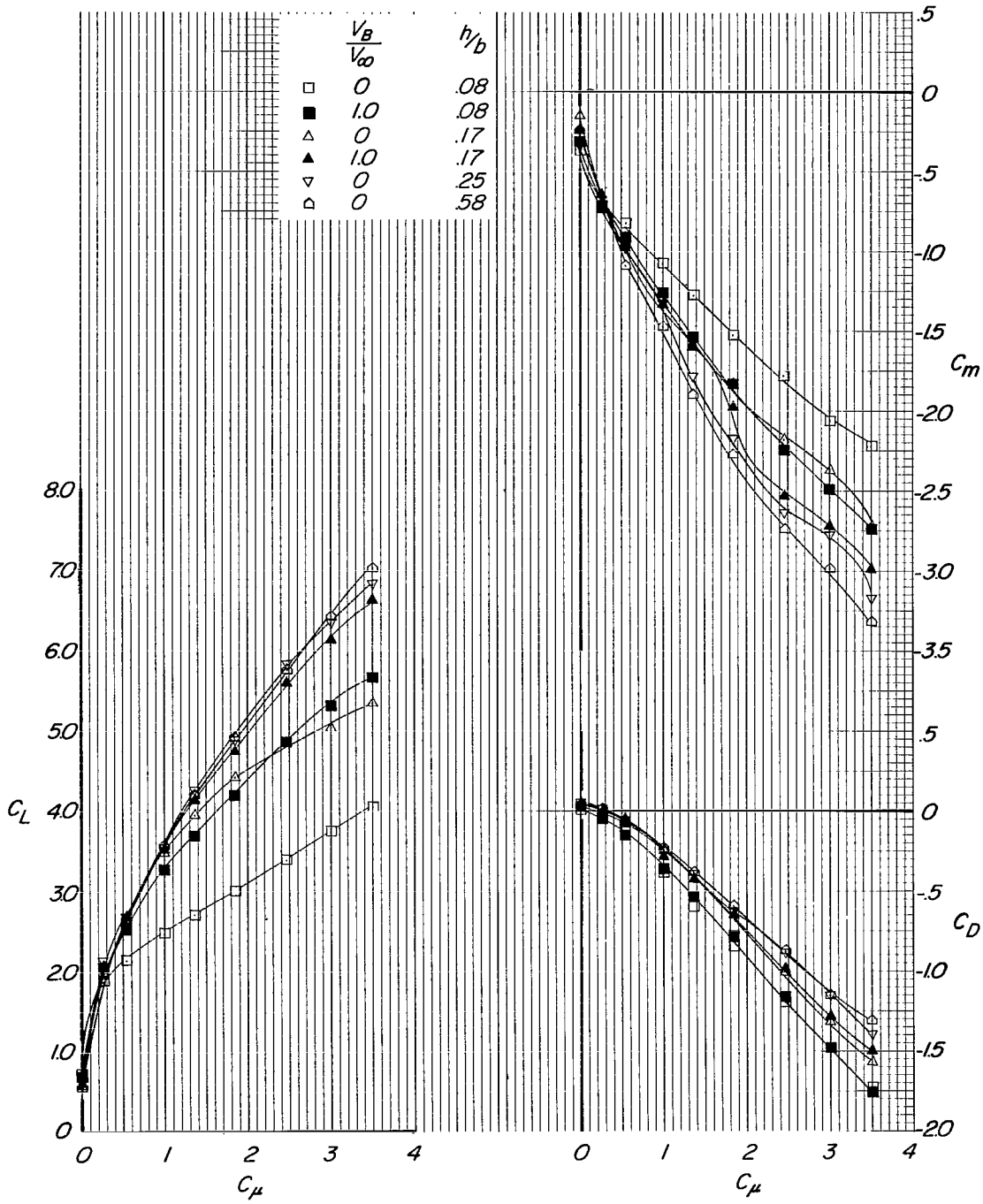

(c) $\delta_f = 45^0$.

Figure 9.- Continued.

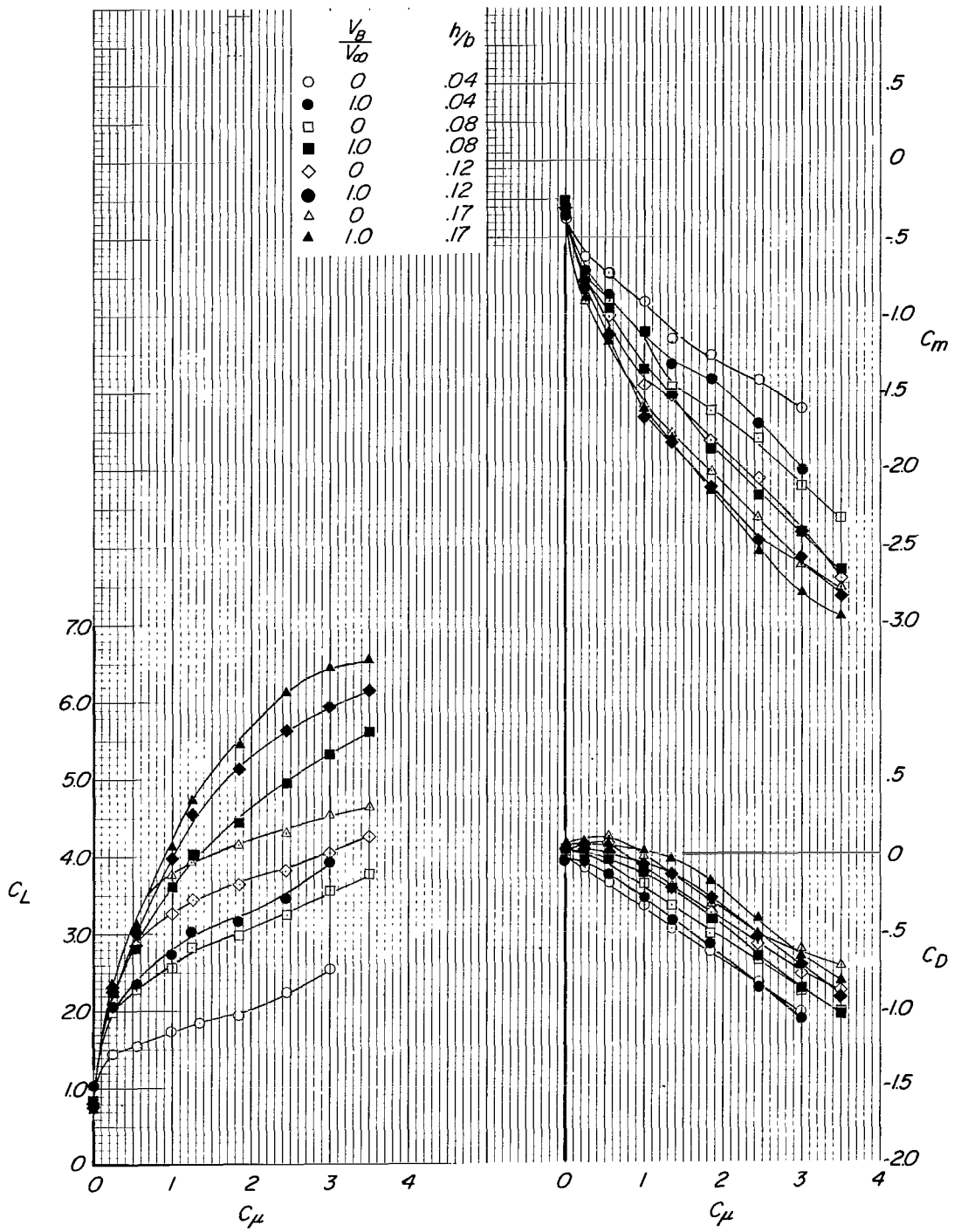

(d) $\delta_f = 60^0$.

Figure 9.- Continued.

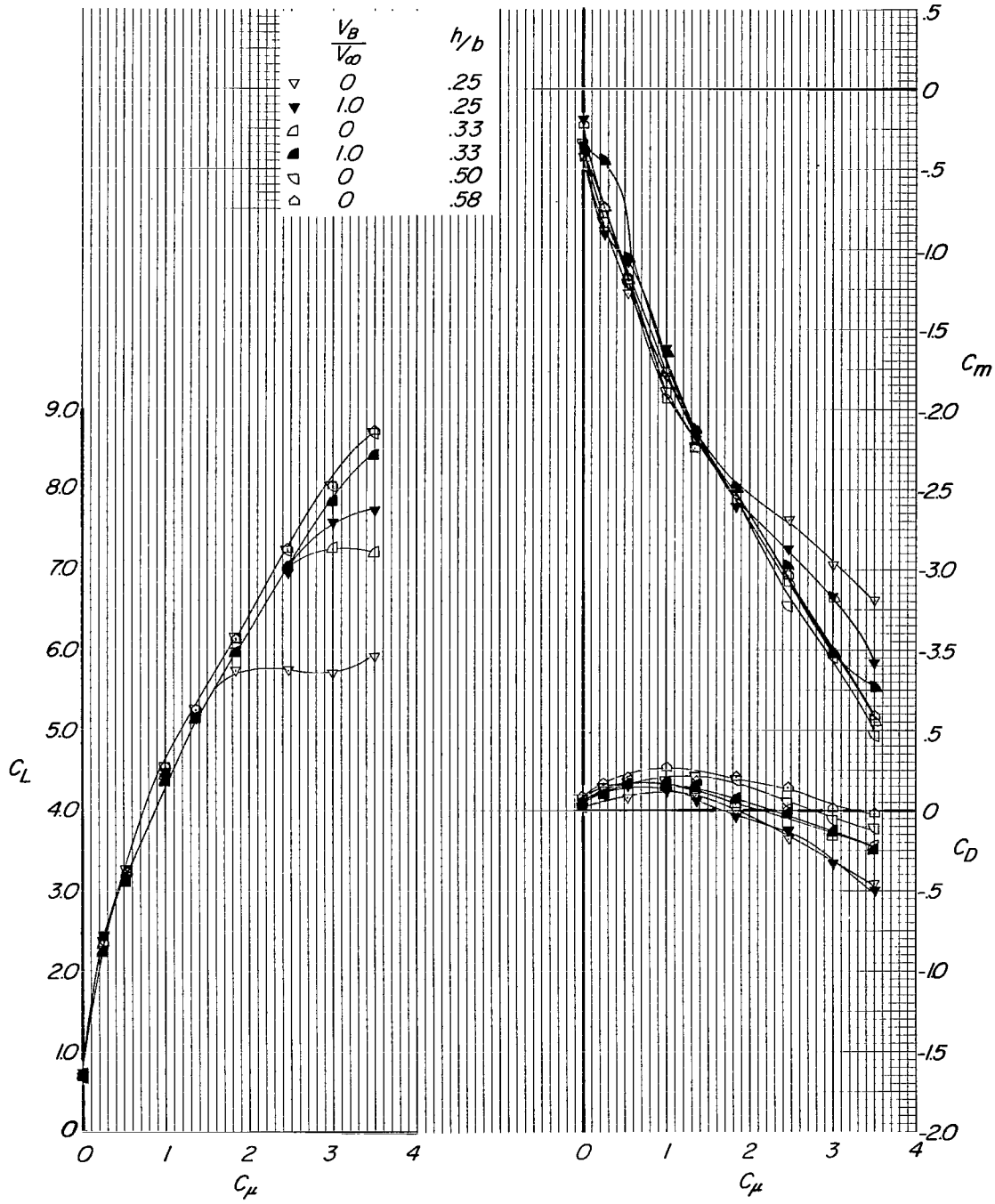

(d) Concluded.

Figure 9.- Continued.

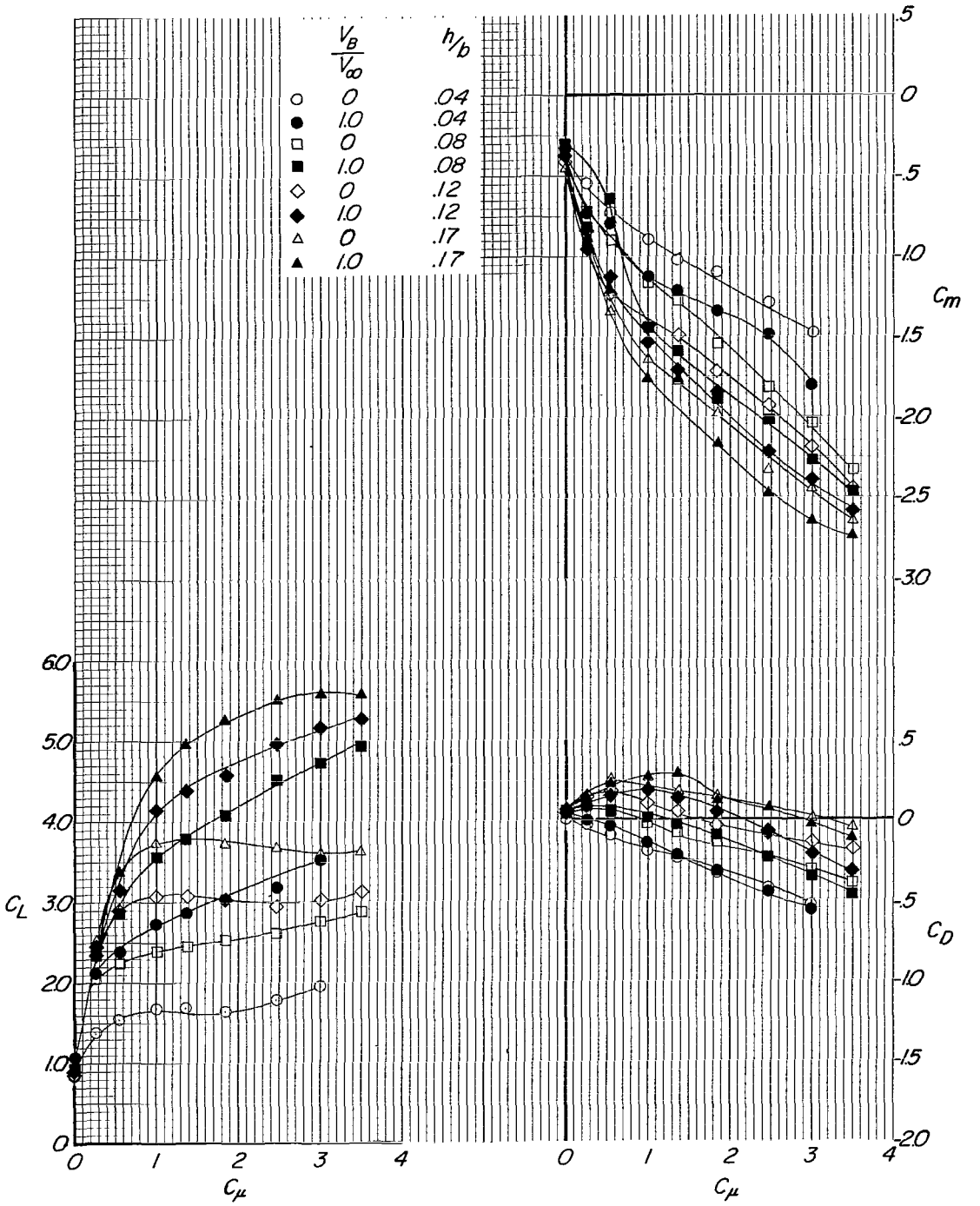

(e) $\delta_f = 75^0$.

Figure 9.- Concluded.

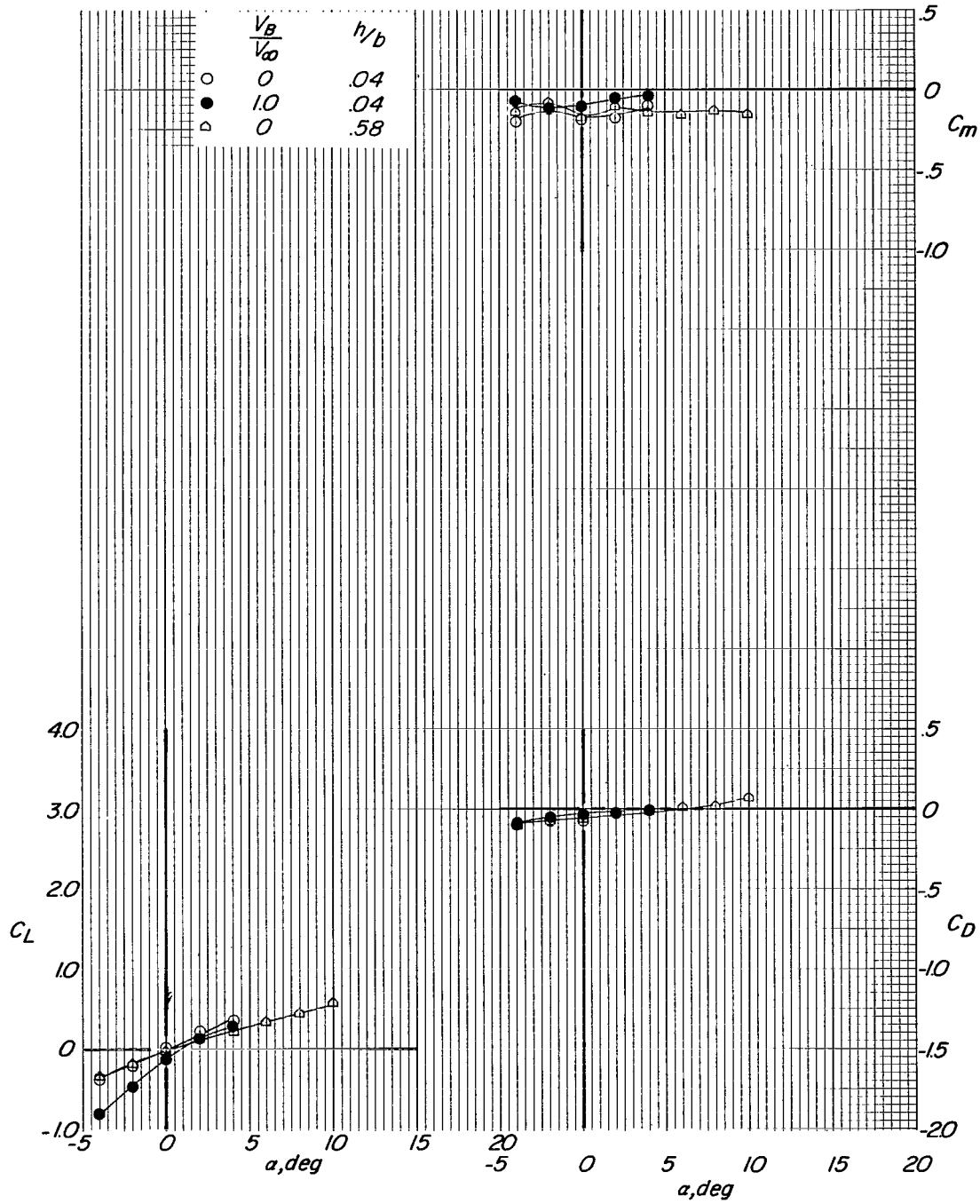

(a) $\delta_f = 0^0$; $C_\mu = 0$.

Figure 10.- Variation of aerodynamic characteristics of unswept airfoil with angle of attack for various heights above moving-belt ground plane.

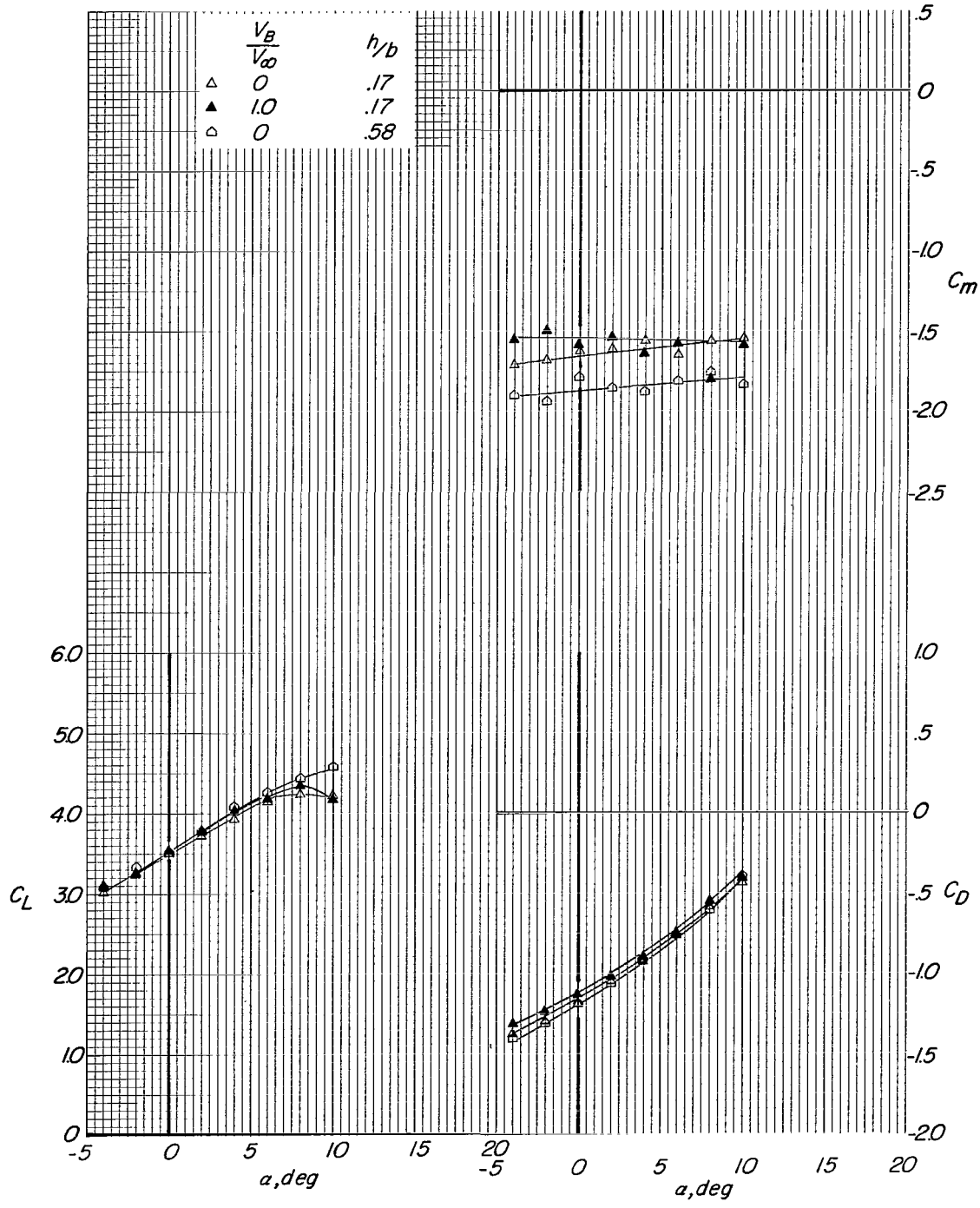

(b) $\delta_f = 30^0$; $C_\mu = 1.8$.

Figure 10.- Continued.

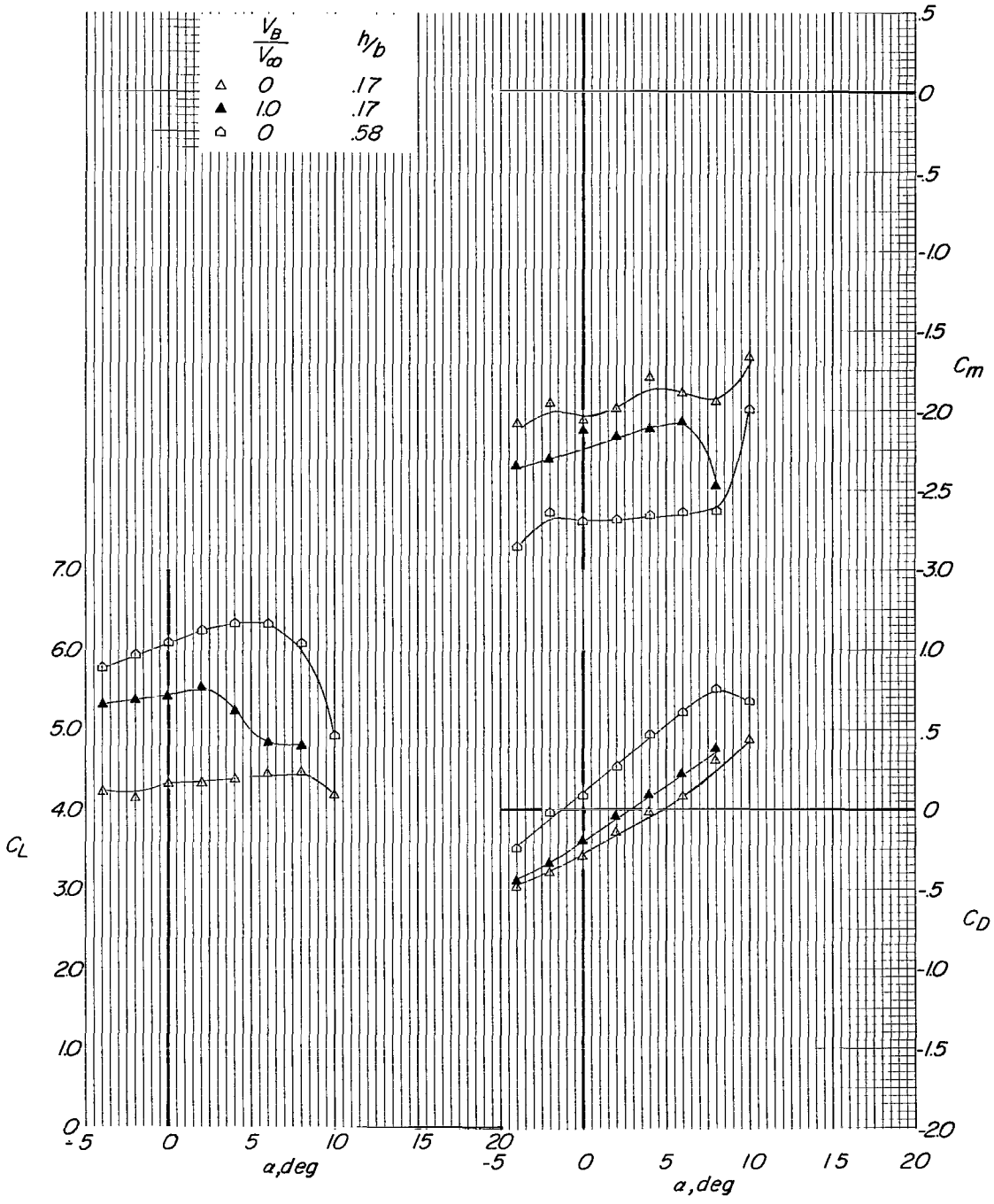

(c) $\delta_f = 60^0$; $C_\mu = 1.8$.

Figure 10.- Continued.

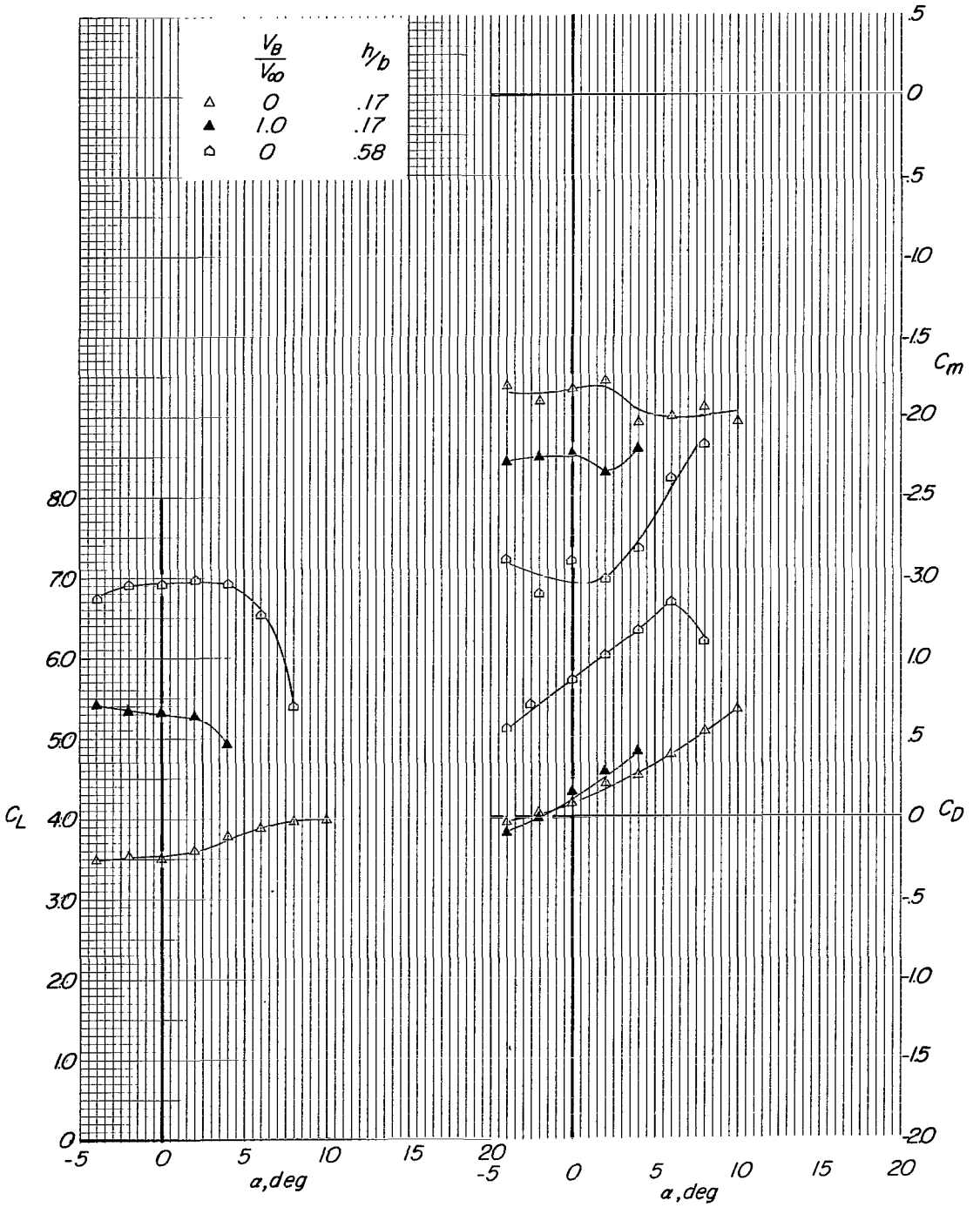

(d) $\delta_f = 75^0$; $C_\mu = 1.8$.

Figure 10.- Concluded.

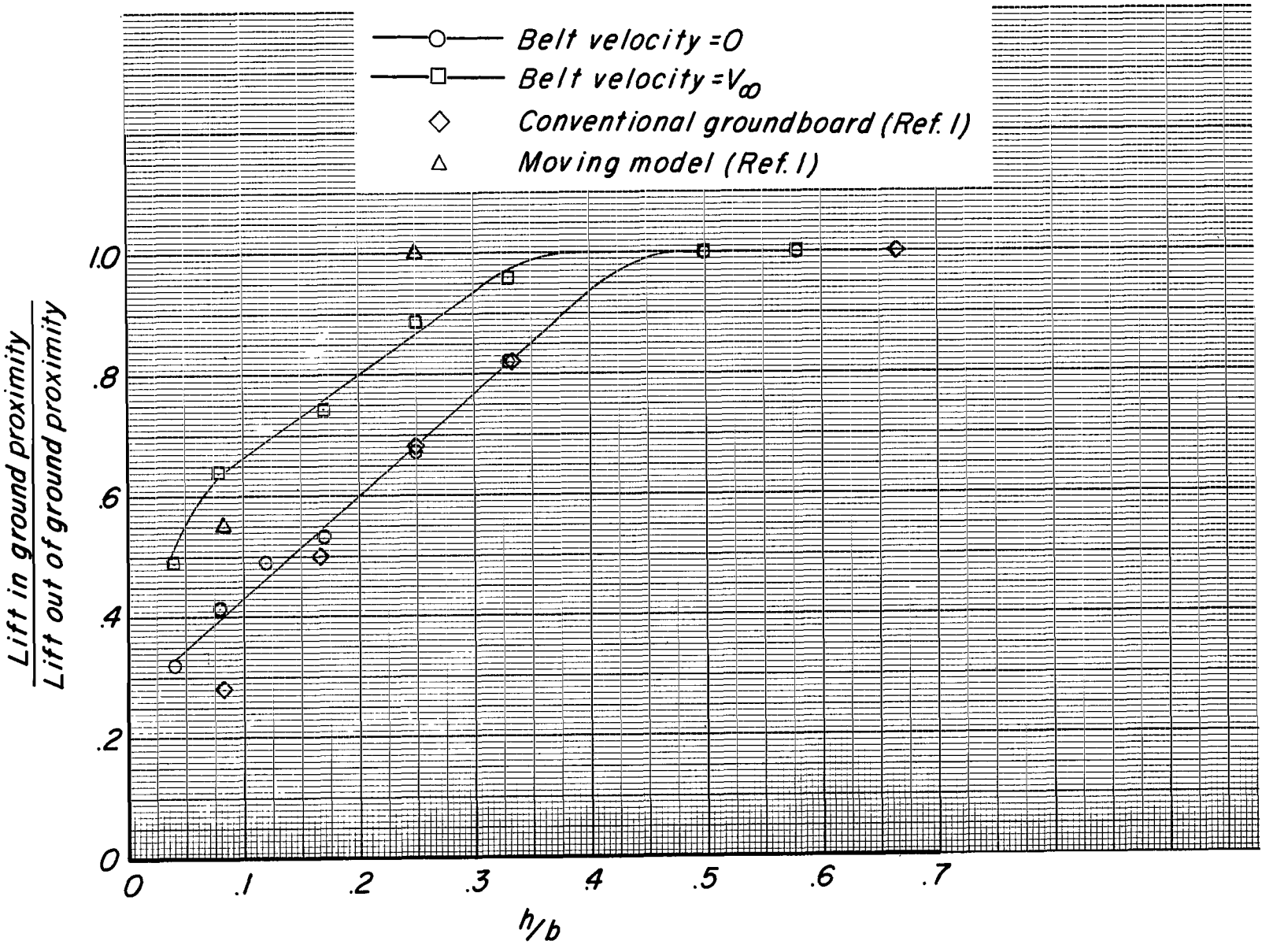

Figure 11.- The effect of ground nearness on lift of unswept wing with blowing flap. $\delta_f = 60^0$; $C_\mu = 3.5$; $\alpha = 0^0$.

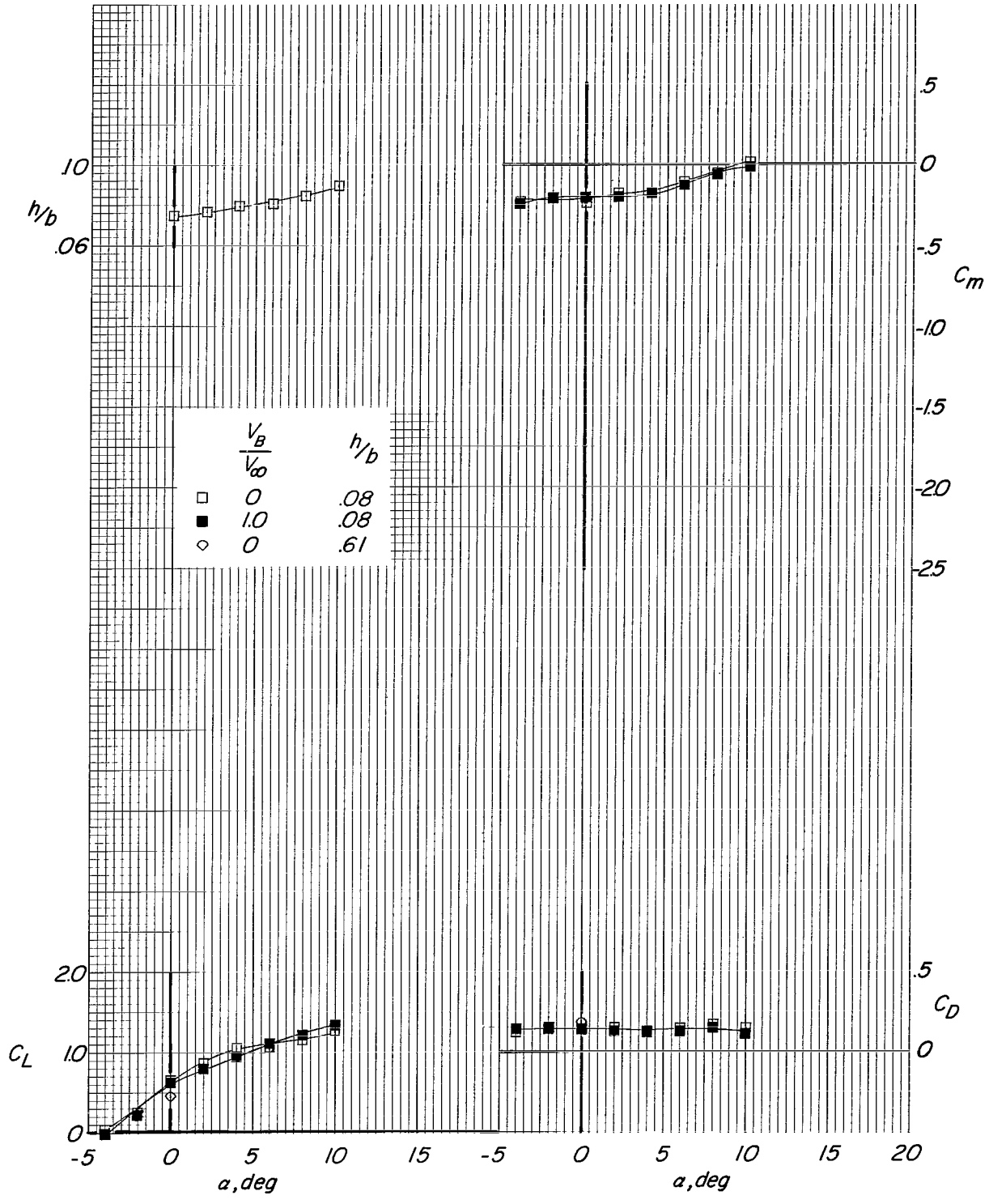

(a) $C_L = 0.50$ for $h/b = 0.61$ at $\alpha = 0^0$.

Figure 12.- Effect of moving belt on longitudinal aerodynamic characteristics of swept model. $\delta_s = 60^0$; $\delta_f = 60^0$.

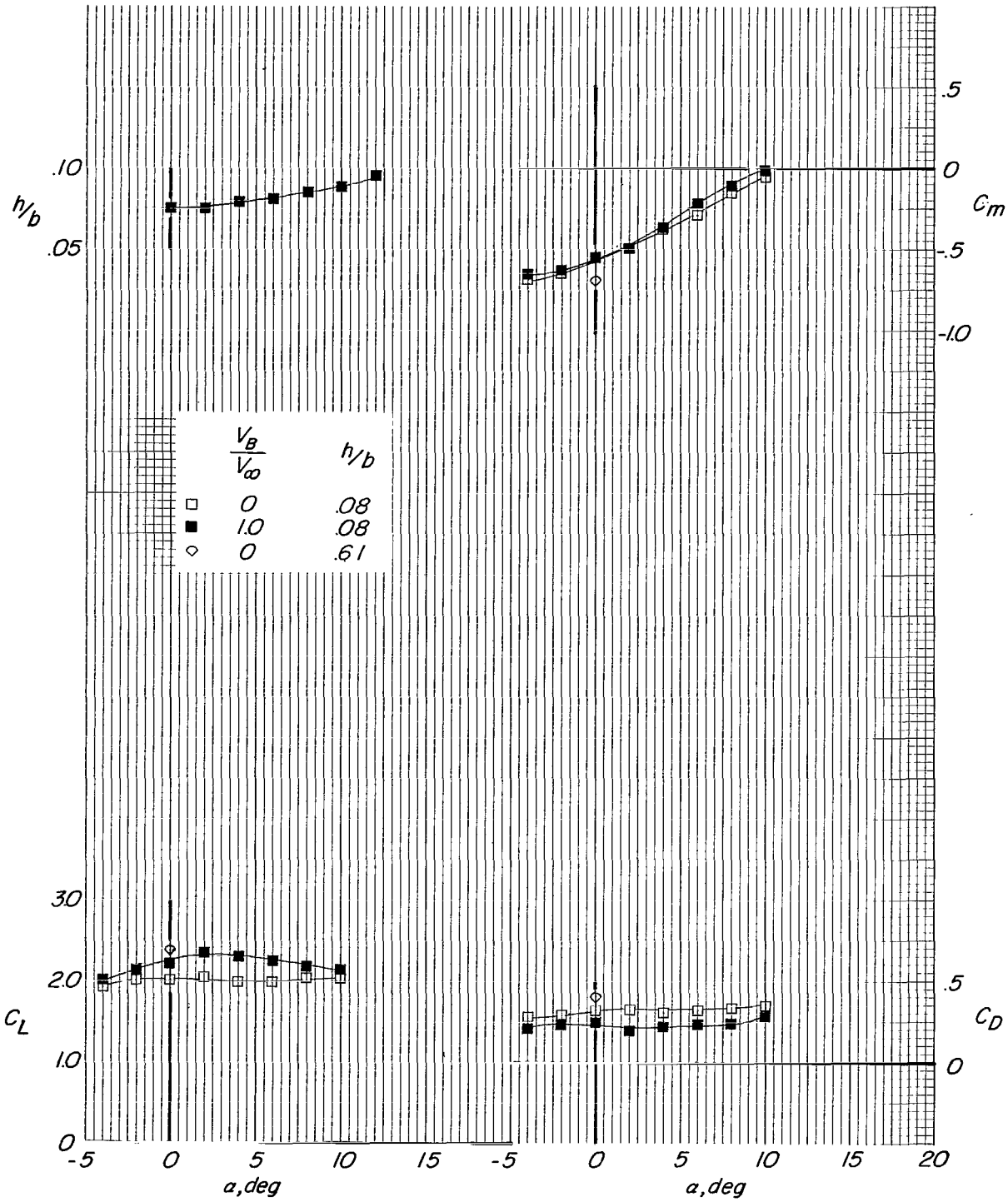

(b) $C_L = 2.45$ for $h/b = 0.61$ at $\alpha = 0^0$.

Figure 12.- Continued.

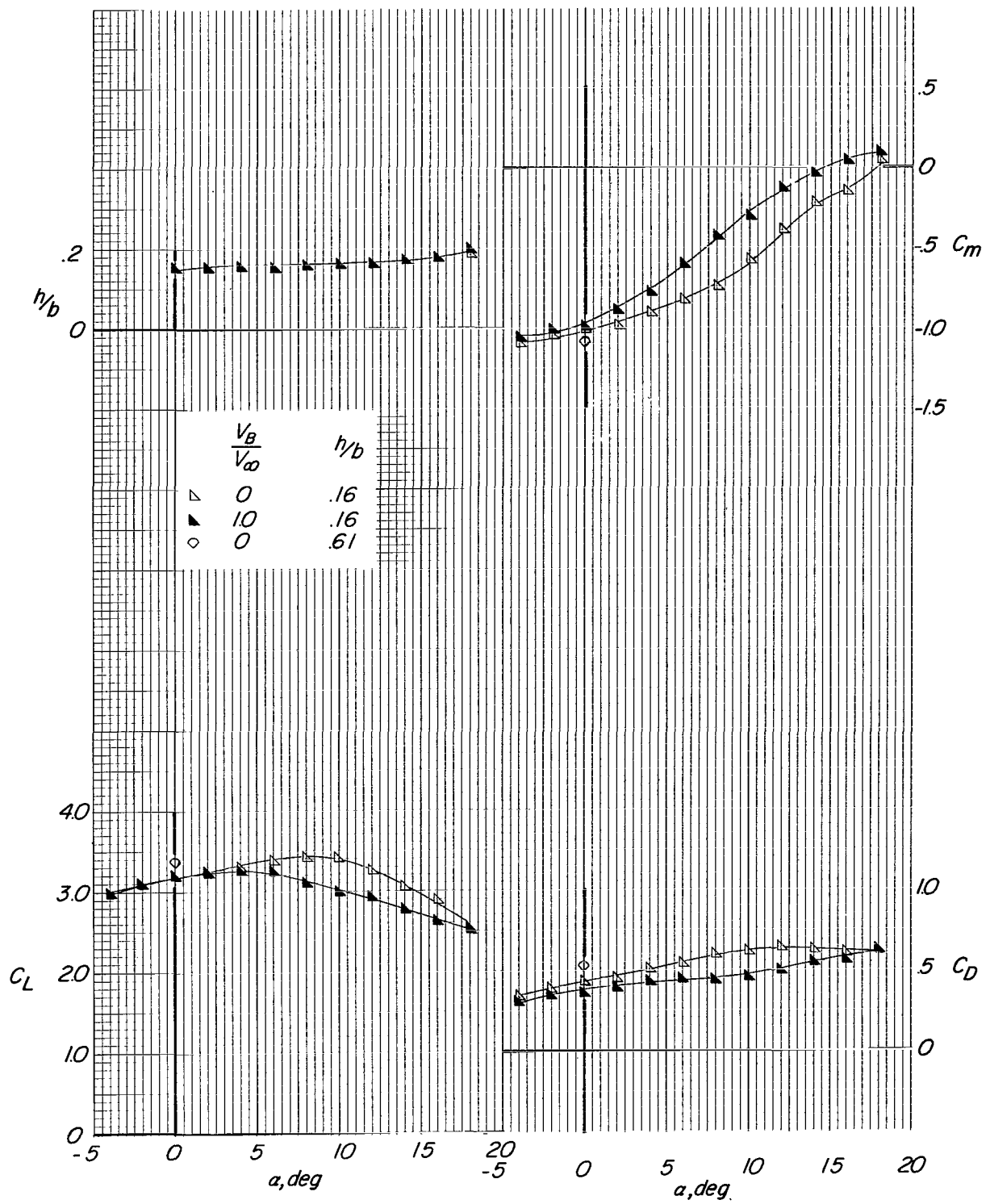

(c) $C_L = 3.35$ for $h/b = 0.61$ at $\alpha = 0^0$.

Figure 12.- Continued.

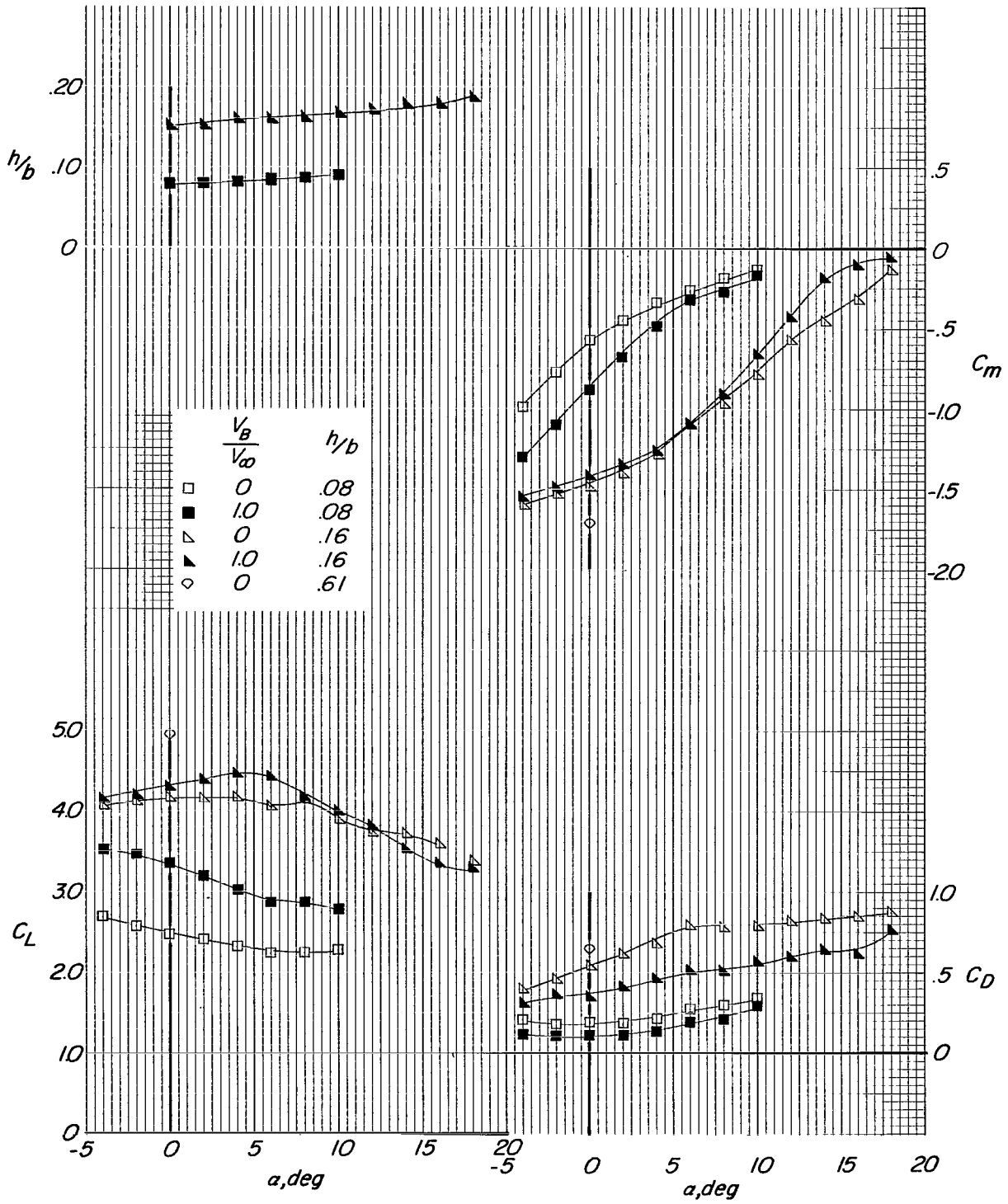

(d) C_L = 4.95 for h/b = 0.61 at α = 0°.

Figure 12.- Continued.

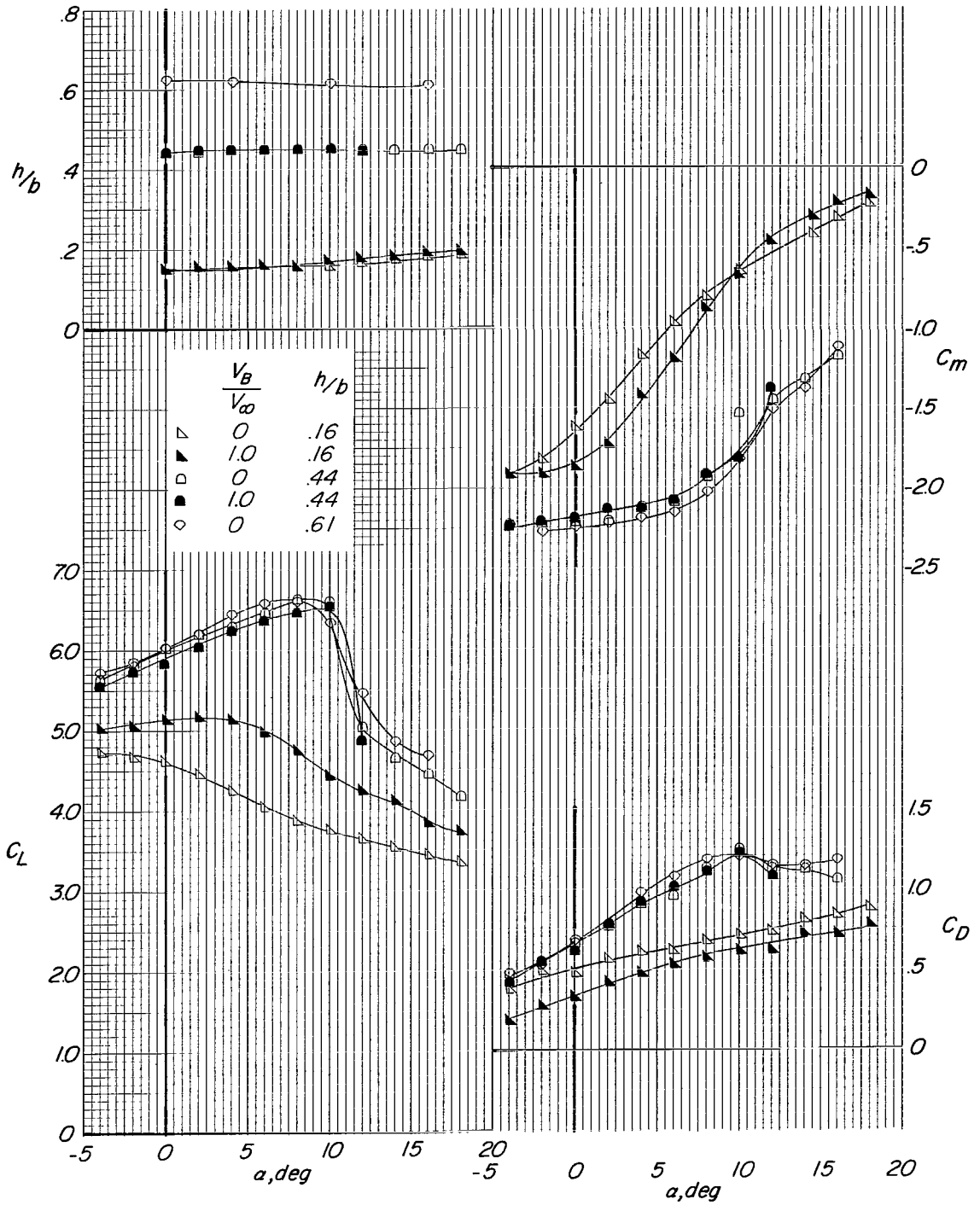

(e) C_L = 6.05 for h/b = 0.61 at $\alpha = 0^0$.

Figure 12.- Continued.

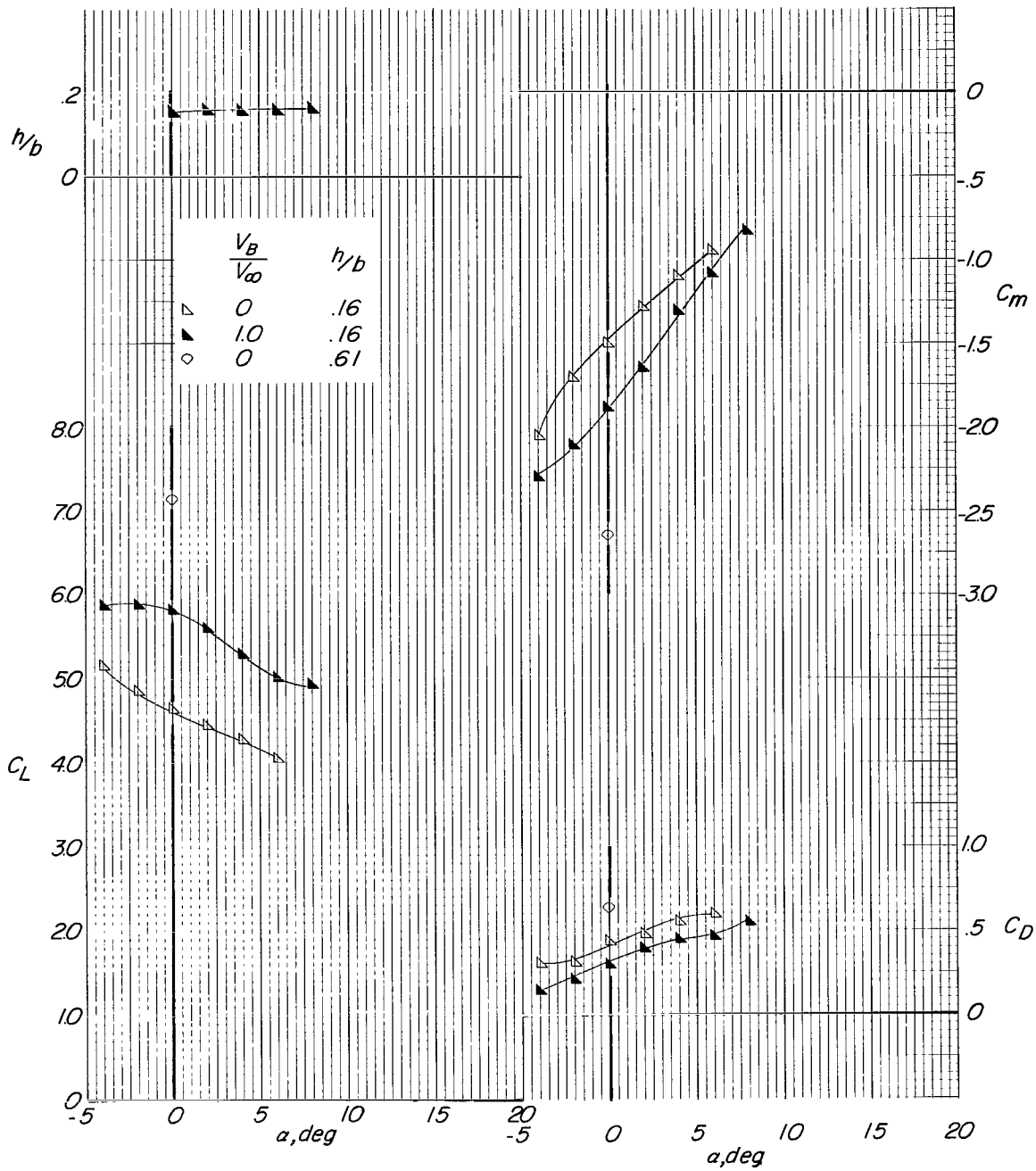

(f) $C_L = 7.15$ for $h/b = 0.61$ at $\alpha = 0^0$.

Figure 12.- Continued.

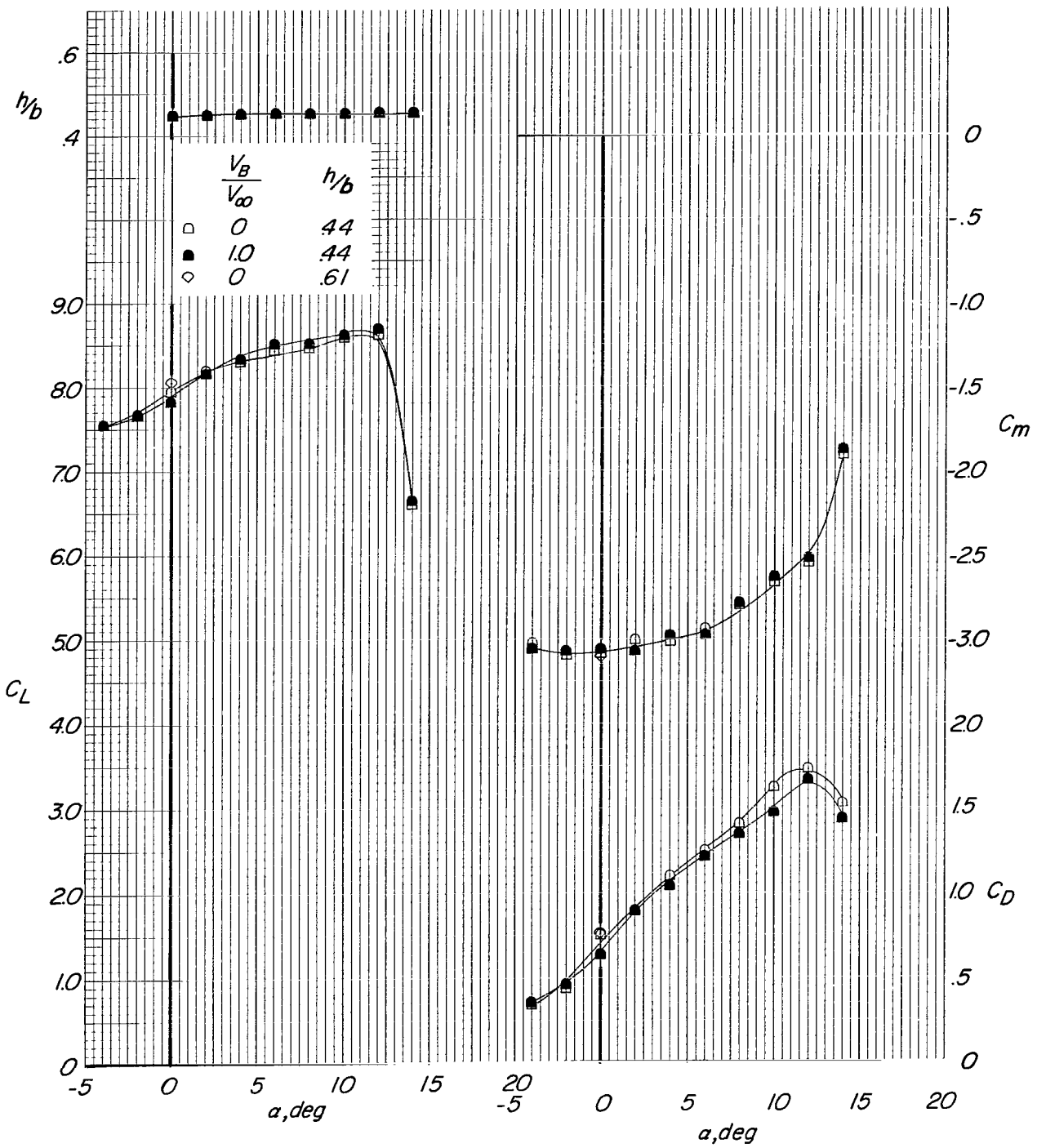

(g) C_L = 8.03 for h/b = 0.61 at α = 0°.

Figure 12.- Concluded.

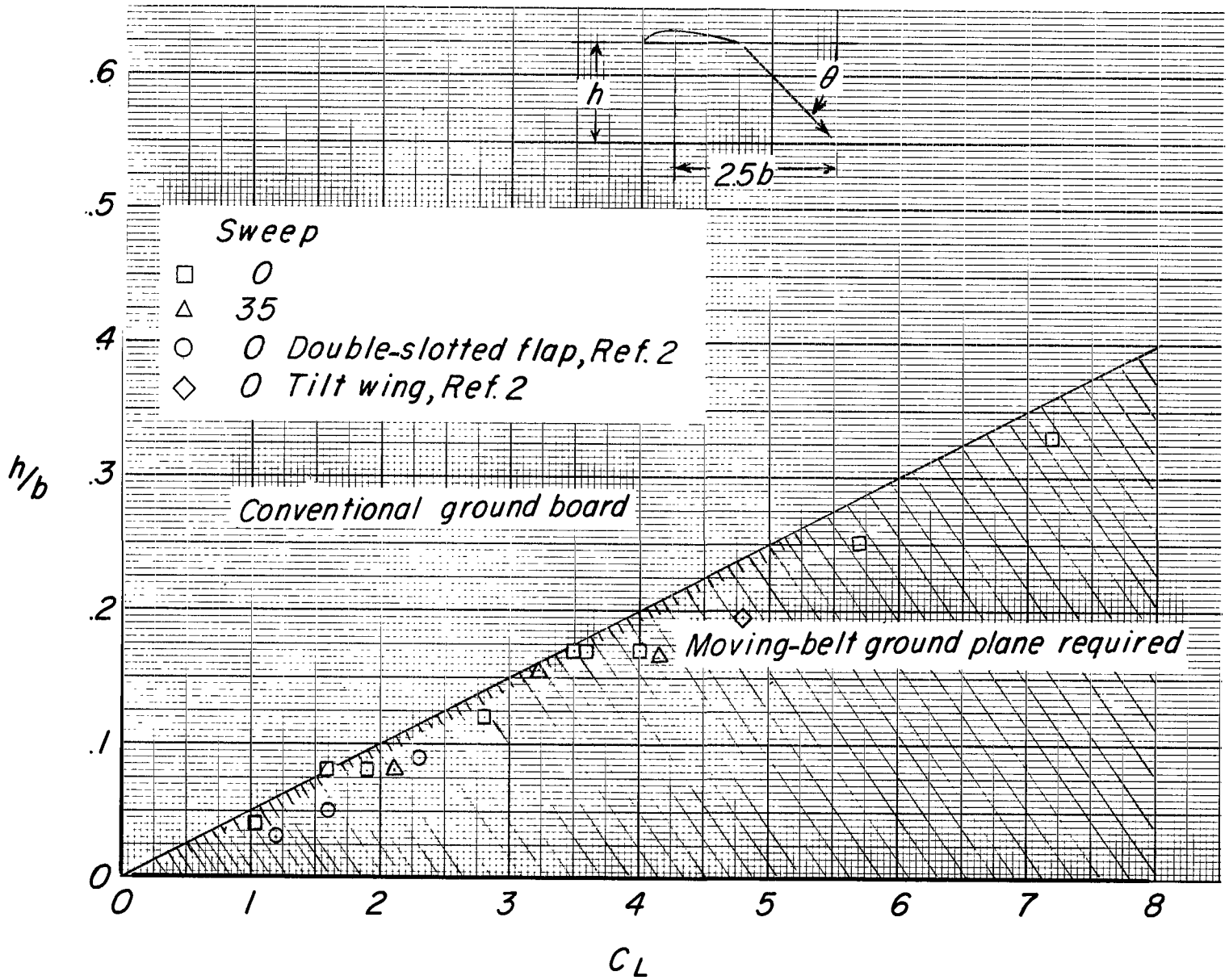

Figure 13.- Graph showing when moving-belt ground plane is required for models with full-span lift devices.

"The aeronautical and space activities of the United States shall be conducted so as to contribute . . . to the expansion of human knowledge of phenomena in the atmosphere and space. The Administration shall provide for the widest practicable and appropriate dissemination of information concerning its activities and the results thereof."

—NATIONAL AERONAUTICS AND SPACE ACT OF 1958

NASA SCIENTIFIC AND TECHNICAL PUBLICATIONS

TECHNICAL REPORTS: Scientific and technical information considered important, complete, and a lasting contribution to existing knowledge.

TECHNICAL NOTES: Information less broad in scope but nevertheless of importance as a contribution to existing knowledge.

TECHNICAL MEMORANDUMS: Information receiving limited distribution because of preliminary data, security classification, or other reasons.

CONTRACTOR REPORTS: Scientific and technical information generated under a NASA contract or grant and considered an important contribution to existing knowledge.

TECHNICAL TRANSLATIONS: Information published in a foreign language considered to merit NASA distribution in English.

SPECIAL PUBLICATIONS: Information derived from or of value to NASA activities. Publications include conference proceedings, monographs, data compilations, handbooks, sourcebooks, and special bibliographies.

TECHNOLOGY UTILIZATION PUBLICATIONS: Information on technology used by NASA that may be of particular interest in commercial and other non-aerospace applications. Publications include Tech Briefs, Technology Utilization Reports and Notes, and Technology Surveys.

Details on the availability of these publications may be obtained from:

SCIENTIFIC AND TECHNICAL INFORMATION DIVISION

NATIONAL AERONAUTICS AND SPACE ADMINISTRATION

Washington, D.C. 20546